Controlling polymer stereochemistry in ring-opening polymerization: a decade of advances shaping the future of biodegradable polyesters

Mathieu J.-L. Tschan, Régis M. Gauvin, Christophe Thomas

Controlling polymer stereochemistry in ring-opening polymerization: A decade of advances shaping the future of biodegradable polyesters

Mathieu J.-L. Tschan,[a,*] Régis M. Gauvin,[a] Christophe M. Thomas[a,*]

[a] Chimie ParisTech, PSL University, CNRS, Institut de Recherche de Chimie Paris, 75005 Paris, France.
E-mail: mathieu.tschan@gmail.com; E-mail: christophe.thomas@chimieparistech.psl.eu

Abstract

This review highlights recent developments in the field of biodegradable polymeric materials intended to replace non-degradable conventional plastics, focusing on studies from the last ten years involving the stereoselective ring-opening polymerization of cyclic esters. This encompasses exciting advances in both catalyst design and monomer scope. Notably, the last decade has seen the emergence of metal-free stereocontrolled ROP for instance, as well as the synthesis and stereocontrolled polymerization of new types of chiral monomers. This study will emphasize recent stereoselective polymerization catalysts and chiral monomers and will focus on stereocontrol quantification, the mechanisms of stereocontrol and their differentiation if reported and studied for a specific catalyst system.

1. Introduction

1.1. Background

The production of fossil-based materials reached 368 million tons in 2020.[1] These materials, once introduced into the market, would end up in the environment, causing serious environmental pollution.[2] In addition, given the depletion of fossil feedstock, the development of biodegradable polymeric biomaterials to replace non-degradable conventional plastics is now a global priority. Several excellent reviews have summarized the challenges, methodology, economics, ecological impact, and recycling of known renewable plastics.[3,4] In order to address these growing problems, much research has been conducted on the synthesis of (bio)degradable polymers and the dramatic progress achieved over the past 30 years in the synthesis, manufacture, and processing of these

materials has led to a wide range of practical applications, from packaging to biomedical devices.

Among the variety of known biodegradable polymers, linear aliphatic polyesters occupy a prominent position, as hydrolytic and/or enzymatic chain cleavage results in o-hydroxyacids which, in most cases, are ultimately metabolized.[5] Polyesters are commonly produced by polycondensation reactions from a diol and a diacid or by ring-opening polymerization (ROP) of cyclic esters. Ring-opening copolymerization (ROCOP) of cyclic anhydrides and epoxides is now also an important methodology to produce polyesters with well-defined microstructure, although no stereocontrolled ROCOP has been reported to date.[6] While the application of condensation polymerization or ROCOP techniques allows access to a broader range of polymer structures than ROP due to a higher accessibility of the monomers involved, the most convenient and efficient method to obtain aliphatic polyesters is the ROP of cyclic esters. Among the various ROP processes, including anionic, cationic, coordination–insertion and organocatalytic, the latter has received increasing attention in recent years.[7]

Polymer properties are highly dependent on the microstructure of the macromolecule and control of stereoselectivity provides materials with precise and finely tuned properties for specific applications.[8] More generally, modulating the tacticity of a polymer gives access to various physico-chemical properties for a single material, and controlling the monomer sequence (or the distribution of chiral centers) within the polymer chain results in a wide range of thermal, mechanical, degradability properties of the material. For instance, highly isotactic polymers have a higher glass transition temperature (T_g), a higher melting temperature (T_m) and a higher thermal stability for superior mechanical properties. In addition, the formation of stereocomplexes between two homochiral polymers or in a stereoblock could lead to novel materials with modified properties.[9] Therefore, achieving stereocontrol from chiral monomers has been the subject of extensive research since the first reports on stereoselective ring-opening polymerization of cyclic esters in the 1980s.[10]

1.2. Scope of the review

This review covers the scientific literature of the last ten years concerning the stereoselective ring-opening polymerization of cyclic esters. Stereocontrolled ring-opening of epoxides and copolymerization with cyclic anhydrides will not be included in the present review.[6c,d,11] Sterecontrolled ROP of *rac*-lactide and β-butyrolactone were

reviewed in 2010[12] but exciting advances were made in this field since then, both in catalyst design and monomer scope. Notably, the last decade has seen the emergence of metal-free stereocontrolled ROP for instance, as well as the synthesis and stereocontrolled polymerization of new types of chiral monomers. Strategies for controlling the relative configuration of main-chain stereogenic centers of chain-growth polyesters are included. This study will concentrate on examining salient examples of recent stereoselective polymerization catalysts and chiral monomers and will focus on stereocontrol quantification, the mechanisms of stereocontrol and their differentiation if reported and studied for a specific catalyst system. Although the emphasis will be on stereochemical control by the catalyst, other important characteristics such as polymerization activity and polymer properties will be included, discussed and contrasted. The review will focus on recent advances in stereocontrolled polymerization studies of *rac*-LA, *rac*-lactones and *rac*-O-carboxyanhydrides (OCAs) to give α-polyesters.

1.3. General information on stereocontrol: mechanism, nomenclature and quantification

We would like to encourage researchers, teachers, students, to read previous reviews concerning the generality of stereocontrolled polymerization of olefin, vinyl and polar monomers.[13] Here we will remind only a few important aspects. The tacticity of a polymer illustrates the relation between adjacent stereocenters. A diad defines the relation between two successive stereocenters, a triad between three stereocenters, a tetrad a sequence of four stereocenters and so on, as illustrated in Fig. 1 where *m* or *i* = iso and *r* or *s* = syndio using the Bovey formalism. Depending on the polymer structure, the different tacticities of n-ads can be detected using various analytical techniques (see below).

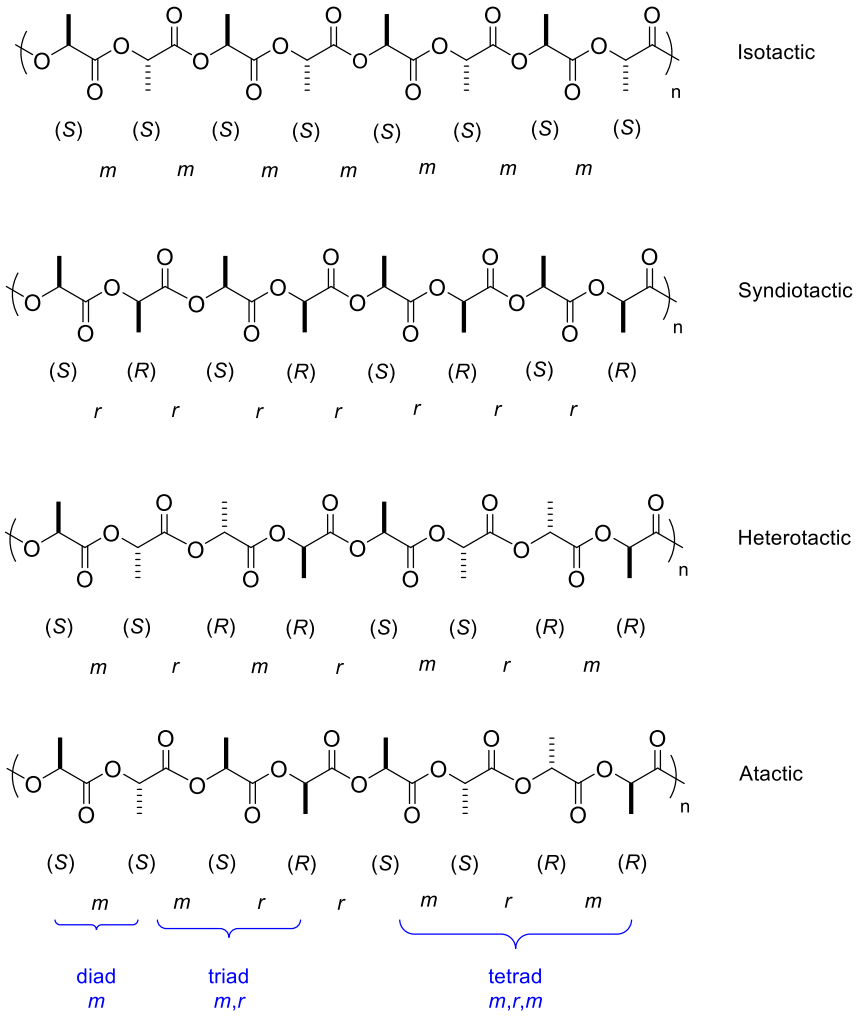

Fig. 1 Common polymer tacticities in stereocontrolled ROP, exemplified with polylactides.

Stereocontrol can be achieved by two different mechanisms: a *chain-end control* (CEC) mechanism or an *enantiomorphic site control* (ESC) mechanism. In a chain-end control mechanism, the chirality of the stereogenic center of the last inserted monomer unit bound to the catalyst determines the chirality of the next monomer to be inserted; this is generally associated with hindered but achiral catalyst systems. By contrast, enantiomorphic site control is demonstrated when the chirality of the catalyst dictates the chirality of the next insertion. However, it is very important to mention that using a chiral catalytic system does not necessarily imply a site control mechanism for stereoselective systems even if enantioselective discrimination (or enantioselection) towards the racemic monomer is observed during the polymerization. Several examples that will be discussed in this review have been reported as stereoselective chiral catalysts operating by a chain-end control mechanism. The main differences arise from the two different types of

stereocontrol mechanisms: In a CEC mechanism, the polymerization rates k_p of the two enantiomers of the monomer M, namely (*R*)-M and (*S*)-M are equal: k_p((*R*)-M) = k_p((*S*)-M). By contrast, in an ESC mechanism, k_p((*R*)-M) ≠ k_p((*S*)-M). Moreover, both mechanisms produce polymers with distinct stereochemical errors; a misinsertion is immediately corrected in a site-control process, but the error is propagated if the chain-end dictates the next insertion.

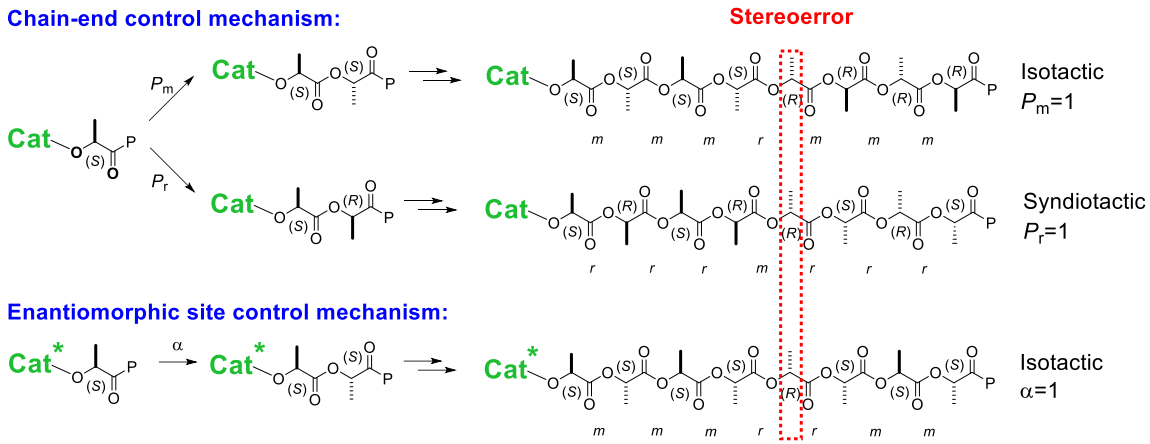

Scheme 1 Chain-End and Enantiomorphic Site Control mechanisms and impact on error insertion as exemplified by PLA synthesis.

In ring-opening polymerizations, the monomers used in stereocontrolled processes are generally chiral and used as a racemic mixture; stereocontrol is achieved by controlling the sequence of the chiral center of the monomers inserted in the polymer chain (Scheme 1). In an enantiomorphic site control process, selectivity is defined in terms of α, the probability that a given enantiomer of the catalyst will preferentially react with one enantiomer of the chiral monomer. Chain-end control is defined in terms of the probability of a *meso* (P_m) or *racemic* (P_r) placement according to the Bovey's formalism (nowadays we tend to replace *meso* with *isotactic* (i) and *racemic* with *syndiotactic* (s)), i.e., the probability of creating a new *meso* or *rac* linkage. When P_m or P_r is equal to 1, it indicates that the polymer is isotactic or syndiotactic respectively. However, when α is equal to 1 or 0, the polymer formed is isotactic and when α tends to 0.5, an atactic polymer is obtained. In some reports, researchers have also renamed α as the probability of *meso*

placement P_m or P_i (probability of isotactic placement). Several techniques can be used to determine the type of tacticity and degree of stereoregularity of a polymer sample. Nowadays, NMR spectroscopy and differential scanning calorimetry of the polymers are efficient techniques to determine and quantify the polymer tacticity, and also to study the influence of stereoregularity on material properties. For chiral polymers, optical rotation and chiral chromatography analysis (high performance liquid chromatography (HPLC) or gas chromatography (GC) for instance) can allow establishing the absolute configuration as well as the degree of enantiomeric purity of the polymer (when the optically pure polymer is available) and of the unreacted monomer, respectively. Undoubtedly, NMR spectroscopy is the most useful and practical method, especially high resolution or quantitative ^{13}C NMR spectrum or homonuclear decoupling ^{1}H NMR spectrum for determining a polymer tacticity and quantify the stereoregularity.[14] The actual NMR sequence or type and nature of observed nucleus strongly depends on the polymer which is being investigated. In many cases, the chemical shifts of different nuclei within the polymer are sensitive to adjacent stereogenic centers, resulting in a fine structure that can provide quantitative information on the polymer microstructure once the chemical shift identities are assigned. The ratio of the peaks corresponding to different sequences of stereocenters in the polymer chain known as diads, triads, or n-ads gives a quantitative measure of the stereoregularity of the polymer. Moreover, the ratio of the peaks can also be used to determine the mechanism of stereocontrol, since the spectra can be simulated using the statistical models. For instance, Scheme 1 shows that isospecific chain-end control mechanisms produce polymers with isolated *r*-diad errors, whereas site-control mechanisms produce polymers with isolated *rr*-triad errors and in a site-control process the tetrad ratios in the polymer follows [*rmr*] = [*mmr*] = [*rmm*] = [*mrm*]/2.[15,16]

2. Stereocontrolled ROP of *meso*- and *rac*-lactide

2.1. Introduction

Poly(*L*-lactic acid) (PLLA) is an important biobased polymer made from 100% sustainable and renewable resources. PLLA has been produced at ~400 ktons in 2020.[1] As lactide can exist as a mixture of three diastereomers the (*S*,*S*)- or *L*-lactide, the (*R*,*R*)- or *D*-lactide and the (*R*,*S*)- or *meso*-lactide, *rac*-LA and *meso*-LA are obtained as side products of the production of the *L*-lactide monomer. The challenge of stereocontrolled ROP of *rac*-LA under industrially relevant conditions for the production of highly isotactic polylactide still remains, mainly due to the high temperature required for the bulk ROP of lactide. This strategy would offer two main advantages: producing crystalline polylactides from impure *L*-LA containing *D*- and *meso*-lactide and also achieving the synthesis of PLA stereocomplexes from *rac*-LA in a potentially industrially viable process. As exemplified on Fig. 2, both the nature of the lactide and of the initiating system can govern the outcome of the ROP process in terms of microstructure and therefore, of thermal properties.

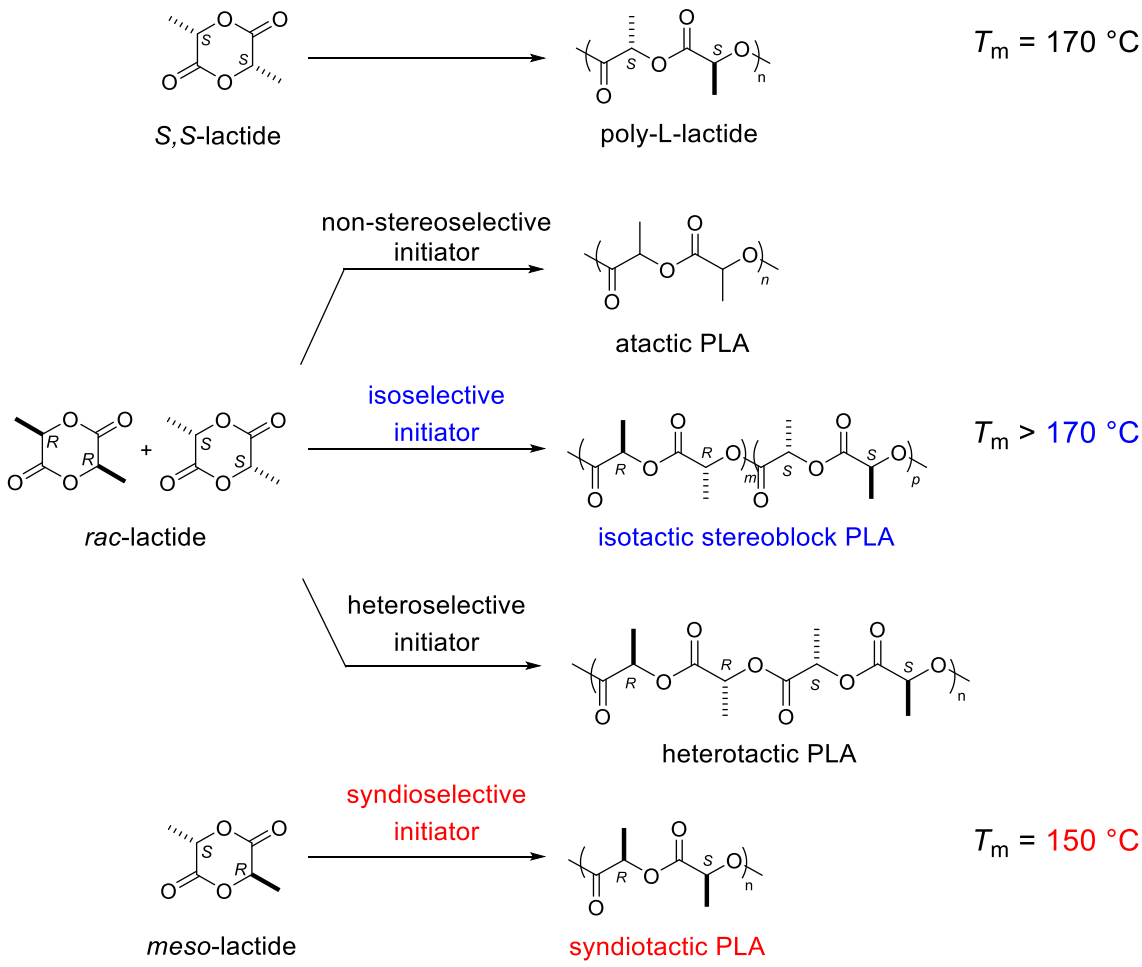

Fig. 2 Interplay between lactide diastereomers and their (stereoselective) ROP into PLA of varying tacticity.

2.2. Organo-/metal-free catalysts

Over the last decade, organocatalysts emerged as promising catalysts for the stereocontrolled ROP of *rac*-LA. Most organocatalysts have the advantage of being water and air-tolerant and allows to obtain polymers that are free of residual metal contaminates, as desired for specific biomedical or microelectronic applications.[7] However, the question of toxicity of organocatalysts is highly dependent on the catalyst used, and it should never be generalized that organocatalysts are always less toxic than their metal counterparts.[17,18] In 2011, Chen *et al*. studied the kinetic resolution (KR) and stereocontrolled ROP of *rac*-LA using cinchona's derivatives such as cinchonidine and *β*-isocupreidine (ICD, **1**, Fig. 3). Cinchonidine was inactive for ROP of lactide and *β*-isocupreidine was found to be enantioselective ($s = k_L/k_D \approx 4$). A modest P_m of 0.75 was reported for a PLA having 10 building units.[19] Surprisingly, the resulting PLA was found to be crystalline and exhibited three melting transition temperatures at 120, 132 and 148 ºC.

Dove and coworkers reported in 2013 an isoselective bimolecular achiral dual organocatalyst consisting in a thiourea and benzylbispidine, an achiral analog of sparteine (**2** and **3**, Fig. 3).[20] The catalytic system is rather active compared to other stereoselective neutral organocatalysts described in this chapter with turnover frequency up to 40 h^{-1} at room temperature. Nonetheless, the P_m values do not exceed 0.77.

Satoh then described the first highly enantioselective organocatalyst for the stereocontrolled ROP of *rac*-LA (enantioselectivity factor $s = k_D/k_L = 28.3$ at 75 °C, $P_m = 0.86$). However, the system exhibited poor catalytic performance and a low degree of polymerization. The chiral (*R*)-binol phosphoric acid (**4**, Fig. 3) preferentially polymerized the *D*-LA monomer to give isotactic PDLA. At 49 % conversion, the enantiomeric excess (ee) of the unreacted lactide was 80 %.[21] One would expect the (*S*)-enantiomer to do just the opposite.

Chen *et al*. reported a detailed study on the KR/ROP of *rac*-LA to produce PLLA and *D*-LA from *meso*-lactide. This innovative strategy was based on the catalytic epimerization of *meso*-LA to *rac*-LA with an extremely active epimerization catalyst DABCO/$B(C_6F_5)_3$ (TOF > 10^5 h^{-1}), followed by subsequent kinetic resolution of *rac*-LA to produce highly isotactic PLLA and highly enantiopure *D*-LA. The chiral ROP catalyst

designed by Chen (**5**, Fig. 3) is the most enantioselective catalyst to date ($s = k_L/k_D = 53$ at 25 ºC; ee = 93% at 50% conversion with 50 eq of monomer, $P_m = 0.88$) for kinetic resolution polymerization of *rac*-LA. Unfortunately, the system only showed an enantiomeric excess ee = 99 % at 83 % of lactide conversion ($s \approx 6$) and the P_m of the PLA prepared also drops to 0.82, suggesting the system loses enantioselectivity and stereoselectivity when the reaction reached high conversions.[22] This catalyst preferentially polymerizes *L*-LA, but it was shown that changing the chirality of the binaphtyl unit from *R* to *S* in the catalyst structure switched the preference in polymerizing the *D*-LA but with lesser enantioselectivity.

Mecerreyes and Cossio reported a densely substituted chiral proline combined with 1,8-diazabicyclo[5,4,0]undec-7-ene (DBU, **6**, Fig. 3) giving a highly isotactic PLA ($P_m = 0.96$) but only for a DP of approximately 25 lactide units.[23] The *endo*- and *exo*-**6** are diastereomers and preferentially polymerize *D*- and *L*-LA respectively but with different enantioselectivity. The PLA obtained at 50 % conversion is crystalline and exhibited a T_m of 165 ºC associated with an enthalpy of 31 J.g^{-1}, that is very similar to PLLA. Thus, the authors claimed that both *endo*- and *exo*-**6** catalysts work by enantiomorphic site control.

In 2018, a revisited study of the enantiopure Takemoto's "TUC" catalyst (**7**) showed the potential of this organocatalyst for isoselective ROP of *rac*-lactide.[24] In fact, the *rac*-TUC was reported to give amorphous PLA from *rac*-LA, but in this study Orhan *et al*. showed that enantiopure TUC gives a semi-crystalline PLA showing a $T_m > 150$ ºC associated with an enthalpy up to 24 J.g^{-1}. The authors studied the mechanism of stereocontrol and showed that both mechanisms of stereocontrol are responsible for the isotacticity of PLA. In this case, P_m and α (referred to as P_m *ESC* in the study) were up to 0.80 and 0.88, respectively. Semi-crystalline PLAs with molecular weights up to 30 kg.mol^{-1} were prepared but the TUC catalyst showed a TOF < 1 h^{-1} when a $[M]_0/[I]_0/[cat]_0$ ratio of 200/1/5 was applied. An interesting feature of the catalyst is that enantiopure TUC was still able to form a semi-crystalline polymer ($T_m = 141$ ºC, $\Delta H_m = 7.6$ J.g^{-1}) at 80 ºC in toluene, unlike many organocatalysts. Unfortunately, in bulk, no stereocontrol could be observed.

Li reported a new cyclic trimeric phosphazene base able to stereoselectively polymerize *rac*-LA at –75 ºC with TOF up to 30 h^{-1} and P_m up to 0.91. Melting temperature of the isotactic block PLA is 191 ºC, characteristic of stereocomplex

morphology.[25] However, no improvement neither in stereoselectivity nor in activity was observed compared to the phosphazene **P$_2$-*t*-Bu** previously reported in 2007.[26] Phosphazene are highly active at RT (TOF up to 30000 h^{-1}) detrimentally to isotacticity. In 2019, Beer and Williams reported achiral rotaxane-based amine-thioureas **9** for isoselective ROP of *rac*-LA.[27] This original system that could be considered as a bulky amine-thiourea due to the presence of the ether-crown macrocycle shuttle produced with low activity an isotactic PLA with a P_m of 0.82 at $[M]_0/[I]_0/[base]_0/[cat]_0$ of 50/1/1/1. Unfortunately, no thermal analysis of the obtained PLA was reported.

Very recently, Taton *et al.* reported an organocatalyst system, combining a chiral commercial aminothiourea TUC **7** and an organic phosphazene base **P$_1$-*t*-Bu**, with both relatively high catalytic activity (TOF ranging from 25 to 50 h^{-1} at room temperature) for an organocatalyst and very high stereoselectivity (P_m up to 0.96, T_m = 187 ºC) providing metal-free and highly crystalline PLA materials.[28] Interestingly, a weaker phosphazene base **P$_1$-*t*-Bu** promotes stereocontrol, probably *via* an mechanism involving hydrogen-bonding with **7**, while the stronger phosphazene base, **P$_2$-*t*-Bu**, provides faster polymerization but less stereocontrol, by a phosphazenium thioimidate ion pair generated *in situ*. As observed with TUC as a single catalyst,[24] a preferential consumption of a given enantiomer of lactide by a given enantiomer of the **7**-phosphazene catalyst was observed. Tschan, Dove et al. reported the design of a tunable bimolecular bifunctional catalyst easily accessible for isoselective ROP of *rac*-LA.[29] The catalyst system is based on substituted chiral and achiral bispidines combined with chiral bis-thioureas. Structural variations of the bispidines (**10a-d**) and chiral **11** were investigated in order to optimize the system. The best catalyst showed promising enantioselectivities in kinetic resolution of *rac*-lactide with selectivity factor up to 6.2. More interestingly, *rac*-LA was polymerized to give a highly isotactic polylactide (α up to 0.88) at almost complete lactide conversion with reasonable activity (TOF up to 6 h^{-1} with a $[M]_0/[I]_0/[cat]_0$ of 100/1/5). Mechanistic studies concluded that this organocatalytic system operates via a stereocontrol mechanism switch from dominant ESC to dominant CEC while lactide conversion increases as Kol's aluminum initiators discussed in section 2.4. The obtained PLAs feature pure stereocomplex morphologies exhibiting a T_m up to 172 ºC and an associated ΔH_m up to 40 $J.g^{-1}$. Interestingly, they showed that the chirality of the thiourea governs the enantioselectivity of the reaction (*i.e.*, which lactide enantiomer will be

preferentially consumed) and that the skeleton of bispidine/binaphthyl molecule is key in achieving stereocontrol.

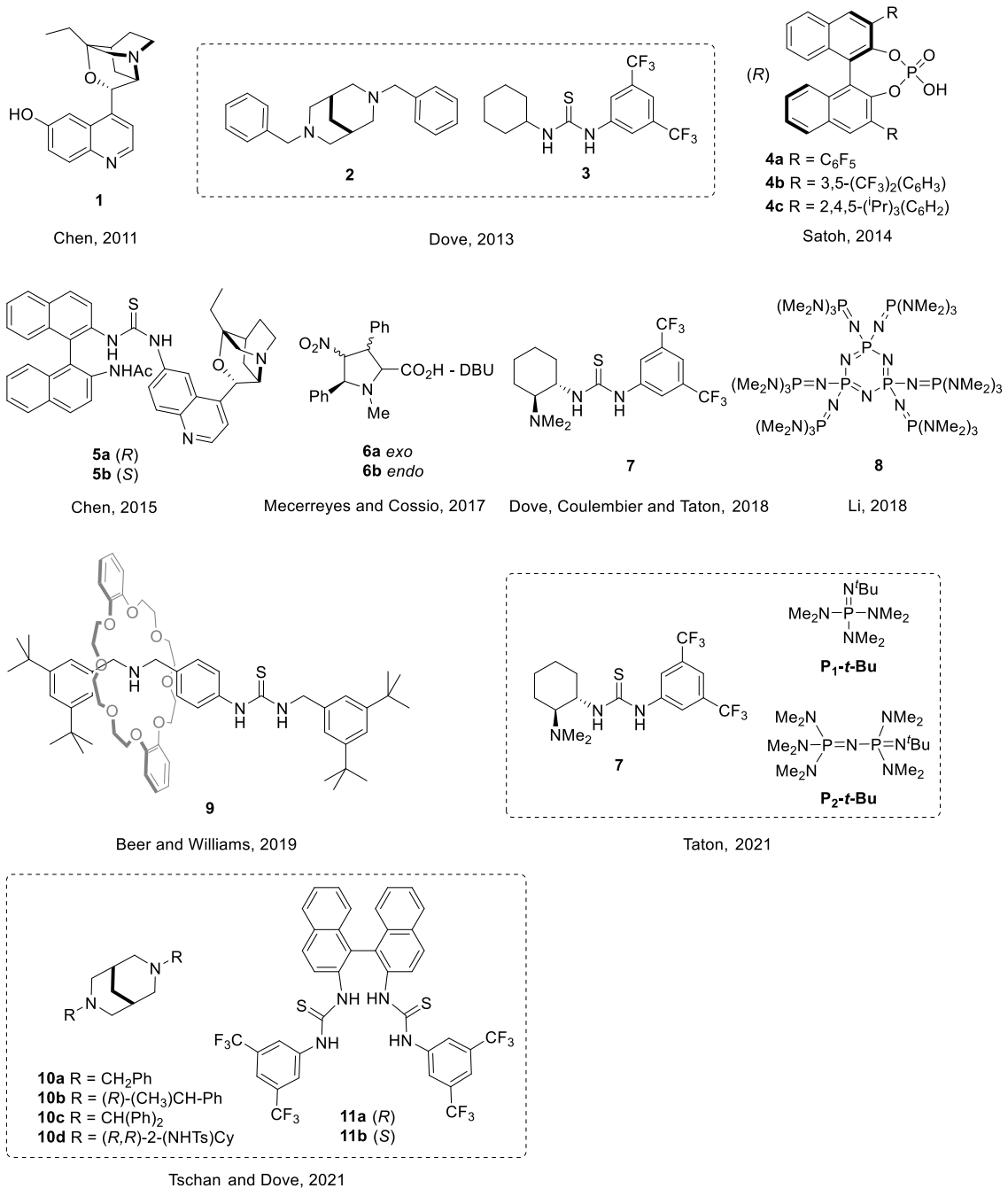

Fig. 3 Metal-free catalysts for stereocontrolled ROP of *rac*-lactide.

In summary, metal-free catalysts have emerged in the last 10 years as promising alternatives to organometallics in the stereocontrolled ROP of *rac*-lactide under practical conditions (RT and above). Indeed, high isoselectivities have been achieved to produce semi-crystalline PLLA by kinetic resolution and PLA stereocomplexes either by CEC or

ESC mechanism. However, this has generally resulted in the preparation of low molecular weight PLA (DP < 50) associated with low activity (TOF < 10 h^{-1}) while operating in environmentally-harmful chloroform or dichloromethane as solvent. This has cast a shadow on the advocated advantages of this metal-free approach, and provides goals to be reached in future systems.

2.3. Alkaline salts as initiators

The stereocontrolled polymerization of *rac*-lactide with alkaline salts was initially reported by Kasperszyk who described the use of ^{t}BuOLi initiator.[30] A heterotactic-enriched PLA was obtained at room temperature. Most of the alkaline salts use in the herein considered context that were reported in the last 10 years were preferentially stereoselective at very low temperature (generally around –70 ºC) and only few accounted for stereocontrol at room temperature. Even if some of them were extremely fast even at –60 ºC, those systems are not viable for large scale ROP in industry. For instance, Wu reported several substituted bulky phenolate and amidinate salts of potassium and sodium crown ether complexes for fast and highly isoselective ROP of *rac*-lactide at very low temperature. Moreover, side reactions or cyclic polymer formation are often observed compromising the chain-end fidelity of the polymers.[31] In 2015, our group reported several lithium salts of bulky salan, salen and NHC analogs of salan (**12**) prepared by *in situ* reaction with *n*-butyl lithium for the controlled synthesis of heterotactic PLA (Fig. 4). The P_r of 0.81 is the highest reported to date for a lithium catalyst at room temperature with good activity (TOF = 300 h^{-1}).[32] The reaction proceeds in the presence of an alcohol initiator via an activated monomer mechanism. Very recently, Liu exploited the work of Waymouth on thiourea anions,[33] and screened the combination of thioureas with potassium methoxide base (**13**) in a 3/1 ratio for the stereocontrolled ROP of *rac*-lactide (Fig. 4). At room temperature the system produces isotactic PLA with a P_m of 0.87 and a T_m of 168 ºC with high activity (TON > 5000 h^{-1}). When ROP is performed at low temperature, a sharp melting transition is observed at 178 ºC with a reported P_m of 0.93 for the PLA obtained with the same initiating system.[34]

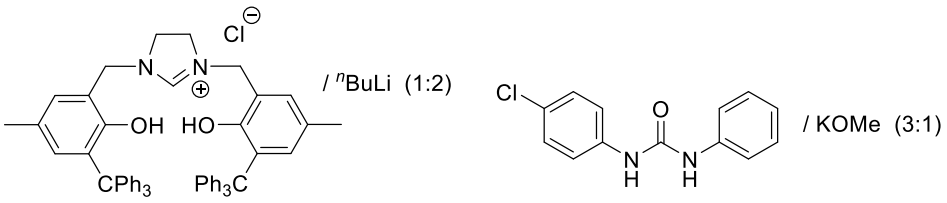

12 **13**

Thomas, 2015 Liu, 2018

Fig. 4 Alkaline salts for stereocontrolled ROP at room temperature.

2.4. Metal-based initiators

Metal initiators for the stereoselective ROP of lactide have been extensively studied. Rather than performing an extensive review on this, we will focus our discussion on selected examples. Our choice will be made on the advances brought to the field by the considered studies, on the catalytic performances of the described systems in terms of activity and/or stereoselectivity (P_m, P_r or $\alpha > 0.8$). The stereocontrolled ROP of *rac*- and *meso*-lactides using organometallic initiators will be classified by metal type when possible.

2.4.1. Aluminum

Spurred by the seminal work of Spassky, aluminum derivatives have been the most employed and studied metal complexes to design stereoselective initiators since the 90's.[35] A plethora of proligands have been designed for the preparation of aluminum initiators, mainly including the Schiff-base motif. As mentioned above, we will include in this section only selected examples, among the numerous reports on aluminum initiators for lactide ROP.[36,37,38] Indeed, complexes featuring salen, salan, salalen, and different amino-phenol, amido-amine proligands with varied denticities (2 to 4) were developed and studied. Since 2010's however, only few examples have achieved high stereocontrol (P_m, P_r or $\alpha > 0.8$).

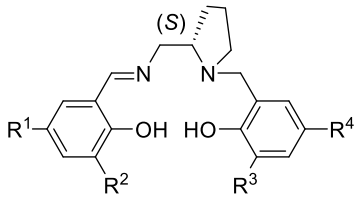

14a: $R^1 = R^2 = Cl$; $R^3 = Ad$, $R^4 = Me$
14b: $R^1 = Me$, $R^2 = Ad$; $R^3 = R^4 = Cl$
14c: $R^1 = R^2 = {}^tBu$; $R^3 = R^4 = Cl$
14d: $R^1 = R^2 = {}^tBu$; $R^3 = R^4 = I$

Kol, 2014

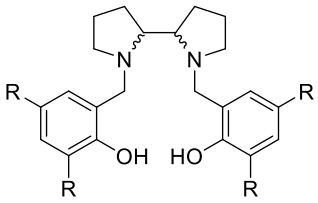

15a: R = H
15b: R = Cl
15c: (*R,R*), R = Me
15d: (*S,S*), R = Me
15e: (*R,S*), R = Me
15f: (*R,S*), R = ^{t}Bu

Jones, 2015 and Kol, 2015

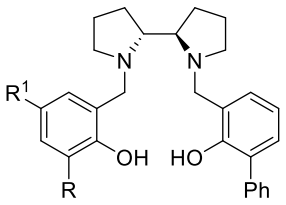

16a: (*R,R*), R = Ph, R^1= H
16b (*R,R*), R = R^1= Cl

Kol, 2019

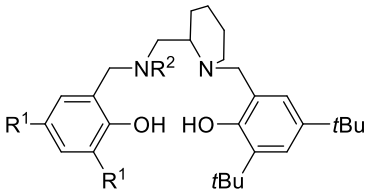

17a: R^1 = tBu; R^2 = H
17b: R^1 = Me; R^2 = H
17c: R^1 = tBu; R^2 = Me

Jones, 2016

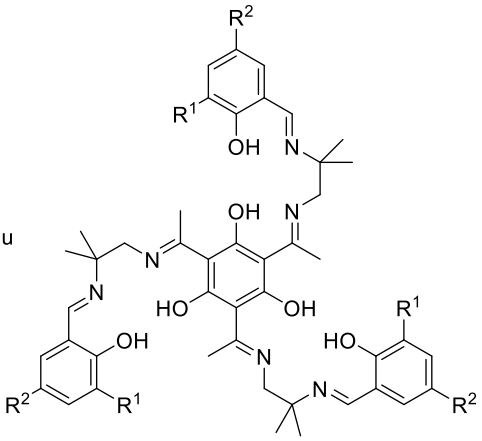

18a $R^1 = R^2 = H$
18b $R^1 = R^2 = {}^tBu$
18c $R^1 = Si(CH_3)_2C(CH_3)_3$, $R_2 = H$

Chen, 2018

Fig. 5 Proligands developed for aluminum complexation.

In 2014, Kol and Lamberti reported a chiral salalen based on aminomethylpyrrolidine to prepare aluminum initiators for the ROP of *rac*-LA (Fig. 5).[39] The enantiopure aluminum complex bearing **14b** and **14c** ligands produced isotactic PLA with a P_m up to 0.82. Kinetic studies showed pseudo first order kinetics for all three lactide stereoisomers (*L*-, *D*- and *rac*-) ROP with **14c**-aluminum-isopropoxide initiator and a selectivity factor s = k_{fast}/k_{slow} of 10. As a consequence of the high s factor value, an ESC mechanism should explain the high isotacticity of the PLA formed. However, the apparent polymerization rate k_{app} for *rac*-LA and D-LA were almost equal. With a pure ESC mechanism operating, one would expect to observe non-first order kinetics with *rac*-LA as one lactide enantiomer should be consumed rapidly and the non-preferred lactide enantiomer converted very slowly, as observed with the Spassky's salen initiator.[35]

Analysis of the optical purity of the produced PLA and of the unreacted *rac*-lactide during the course of the polymerization revealed less enantio-enrichment for PLA and lactide than expected from the kinetics experiment. This behavior suggested that during the ROP of *rac*-LA, CEC is the prevailing mechanism of stereocontrol with a marked influence of ESC at low conversion producing a new type of microstructure for PLA: a gradient isotactic multiblock PLA consisting of *D*- and *L*- lactide of gradually exchanging lengths. These PLAs were semi-crystalline, exhibiting a sharp melting transition around 160 ºC in the first heating scan of the DSC analysis.

Chiral bipyrrolidine based salan decorated with different substituents on the two phenolic units were reported separately by Kol[40] and Jones.[41] Different stereoisomers of the proligand were studied, the (*R*,*R*), the (*S*,*S*) and the meso (*R*,*S*) forms. Thus, Kol reported the aluminum initiators of **15a** and **15b** for ROP of *rac*-LA (Fig. 5). In such complexes, the enantiopure proligands formed a single diastereoisomer. The authors claimed that the (*R*,*R*)-ligand formed the diastereomeric complex with the (*S*,*S*)-nitrogen configurations upon coordination and vice-versa. This statement was confirmed by a single set of signals in the ^{1}H NMR of the complexes and by the molecular structure of a bulky derivative of **15** with *ortho*- and *para*-*t*-butyl substituents on the phenol arms, as shown by single crystal X-Ray analysis. Initiators derived from enantiopure **15a** produced slightly isotactic PLA from *rac*-LA. The use of a racemic mixture of complexes decreased the previously observed isotacticity, probably due to the polymer chain exchange mechanism between the two aluminum enantiomers (*R*,*R*)(S_N,S_N) and (*S*,*S*),(R_N,R_N). In contrast, the chloro-derived ligand **15b**, used as its enantiopure form, afforded non-stereoselective initiators for the ROP of *rac*-lactide; atactic PLA was obtained with a rather low k_{app}. However, when the racemic mixture of aluminum complexes was used as initiators, a highly heterotactic PLA was produced (P_r up to 0.98 at 50 ºC in toluene) with a k_{app} ~7 times higher than that of the enantiopure initiator. Kinetic studies showed a first order dependence on lactide concentration, as expected, but also a second-order dependence on aluminum initiators. The authors thus proposed a mechanism based on activation by polymeryl exchange between diastereomers of dormant initiator, depending on the chirality of the initiators and the polymer chain-end. Due to the low steric hindrance of the proligand substituents in **15a** and **15b**, it could also be proposed that this results from the formation of dinuclear aluminum initiators in which the *meso*-version of the dinuclear complexes is the active and hetero-selective species for the ROP of lactide via CEC. The second order dependence on aluminum also supported such a hypothesis.

Jones studied the chiral proligands (*R*,*R*)-**15c**, (*S*,*S*)-**15d** and the meso (*R*,*S*) **15e-f**. It was found that the enantiopure ligands afforded non-stereoselective aluminum initiators, while the meso ligand formed heteroselective initiators (P_r up to 0.87 at 70 ºC in toluene). Recently, Kol proposed a variation of this scaffold, introducing proligand system **16**, where phenol units substitution could either afford C_2-symmetric **16a** or C_1-symmetric **16b** (Fig. 5).[40b] In this study, DOESY NMR experiments and molecular structure of the different aluminum complexes tend to confirm a mononuclear species both in solution and in the solid state. As reported previously, enantiopure ligands formed a single enantiopure diastereomer aluminum complexes. For the polymerization of *rac*-lactide, enantiopure initiators failed in producing highly tactic PLA materials. However, the racemic initiators derived from **16a** and **16b** produced highly heterotactic PLA with a P_r of 0.99 and 0.93 at 50 ºC respectively. These initiators were further investigated for the stereocontrolled ROP of *meso*-lactide. The enantiopure initiator showed better stereocontrol for the synthesis of highly syndiotactic polylactide, with the less bulky proligand **16b** affording the most syndioselective initiators. The syndiotactic PLA obtained featured a T_m of 153 ºC and a high crystallinity (ΔH_m = 56 J.g^{-1}). Jones reported the use of a series of aluminum initiators based on salan proligands **17a-c** for the ROP of *rac*-lactide in solution and in bulk (Fig. 5).[42] An isotactic-enriched PLA (P_m up to 0.81) was obtained in solution. This isotacticity appeared to be maintained in bulk conditions. However, the thermal properties of the obtained materials were not reported. High temperature (180 ºC) and immortal polymerization conditions (monomer/initiator/transfer agent: 3000/1/10) were also tested. Although the polymerization was still controlled, the isotacticity of the polymer was dramatically reduced.

As a final example in this section, Chen developed a family of C_3-symmetric *tris*-salen proligand scaffolds. These were exploited to prepare trinuclear aluminum complexes.[43] Most interestingly, using an initiator based on proligand **18c**, the resulting PLA showed a P_m value up to 0.98 and a T_m of 220 ºC (Fig. 5). To date, this is the highest melting temperature reported for an isotactic PLA stereocomplex obtained from *rac*-lactide.

2.4.2. Zinc- and magnesium

Zinc and magnesium in their +2 oxidation state feature similar chemistry, while displaying occasionally distinct catalytic reactivity.[44] In the context of ROP initiators design, these two metals are frequently compared, in combination with the same ligand sets, as will be exemplified below.

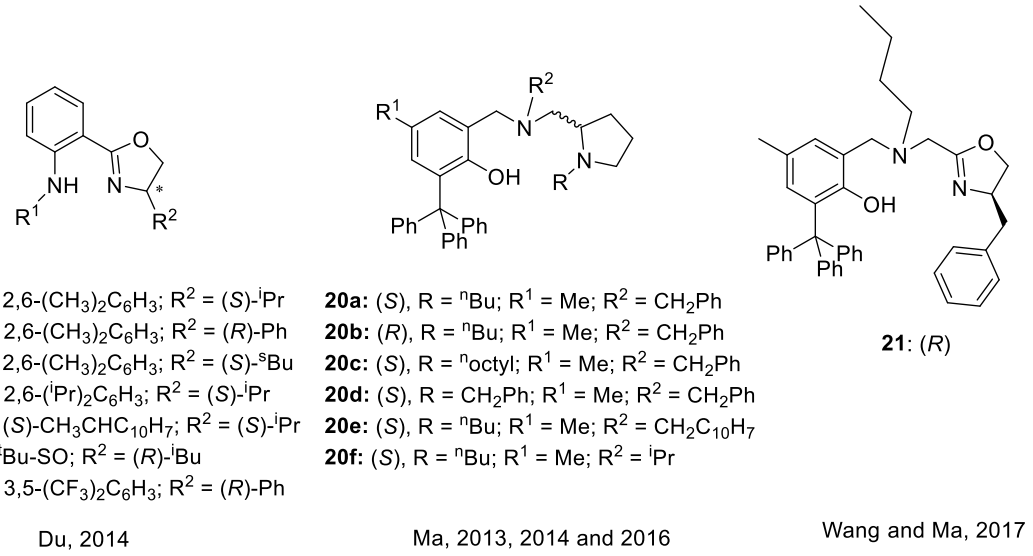

Fig. 6. Proligands developed for zinc coordination

Du reported zinc initiators bearing easily accessible chiral amine oxazoline bidentate ligands **19** for the isoselective ROP of *rac*-lactide (Fig. 6).[45] The initiators were prepared from $Zn[N(SiMe_3)_2]_2$ to give the corresponding L-Zn-$N(SiMe_3)_2$. Due to the slow initiation step *vs*. propagation from the bulky amido group and to transesterification side-reaction, the molecular weights of PLA were higher than expected and $1.05 < Đ < 1.32$. Unfortunately, alcoholysis of the amido initiating group in an effort to improve the ROP initiation step by generating an alkoxide initiator proved unsuccessful, as both the proligand and $Zn(OR)_2$ were also formed upon alcohol addition. With ligand **19a**, a highly isoselective zinc initiator was obtained: P_m values of 0.90 and 0.77 were obtained in solution at 0 ºC and in bulk at 130 ºC, respectively. The zinc initiator based on **19g** afforded the highest isotacticity reported for a zinc initiator at room temperature: P_m reached 0.91 and the resulting PLA exhibited one of the highest melting transition temperatures (T_m = 212 ºC) reported to date for a polylactide from *rac*-lactide. Du also studied the mechanism of stereocontrol, showing that the initiators have no marked preferences for the ROP of one of the two lactide enantiomers ($s = k_{fast}/k_{slow} \sim 1.6$) and that the high isotacticity does not result from an ESC mechanism. Therefore, they postulated a CEC mechanism, even though the ratio of [*rmm*] and [*rmr*] tetrads did not

match the expected value. This is probably due to the observed transesterification side-reaction.

Ma reported interesting studies on the stereocontrolled ROP of lactide using amine-pyrrolidine-phenol catalytic systems.[46,47,48] Numerous structural and electronic variations were made on the ligand to optimize the stereoselectivity of the corresponding initiating systems. In the first report, Ma observed an interesting stereoselectivity switch when comparing the *ortho*- and *para*- phenolic moiety substituents: using two chloro or an *o*-trityl and a *p*-methyl (**20a**) resulted in the production of slightly heterotactic (P_r = 0.60) or isotactic-enriched (P_m of 0.81) polylactide, respectively (Fig. 6). This effect was also observed previously by Gibson.[49] The zinc initiator bearing ligand **20a** produces high molecular weight PLA with good activity (TOF = 140 h^{-1}). The highest isotacticity was obtained at –38 ºC, and the polylactide obtained featured a T_m of 166 ºC. Upon coordination to zinc, these ligands led to the formation of "chiral at metal" zinc complexes of the type (N,O,N')-Zn-[$N(SiMe_3)_2$]. Since the ligands themselves are chiral and were prepared as pure (*R*) or (*S*) enantiomers, the diastereomeric forms of both complexes could be observed and their diastereomeric ratio estimated. With ligands **20a,b,c,e**, only one diastereomer was formed and the molecular structure was determined by single crystal X-ray structure analyses. With a (*R*)-ligand, the (R_L,S_{Zn}) complexes were formed and vice-versa. Ligands **20a** and **20b** afforded the most isoselective zinc initiators of the study. Alcoholysis of the amido group to generate the corresponding alkoxide species resulted in higher polymerization rates and enhanced molecular weight control. The enantiopure initiators derived from **20a** and **20b** showed a selectivity factor of up to 4 toward the lactide enantiomers, supporting an ESC mechanism. However, ^{1}H homodecoupling NMR experiments revealed a tetrad distribution in better agreement with a CEC mechanism. No change in polylactide tacticity and reaction rate could be observed when using the racemic mixture of initiators (**20b**, S_{Zn}) and (**20a**, R_{Zn}). A hypothetical mechanism of CEC and ESC cooperation was proposed based on kinetic and reactivity studies, and on characterization of zinc model complexes with (*S*)-methyllactate and lactides.

Wang and Ma reported an optimized version of the aminophenol ligand systems by substituting the pyrrolidine fragment with an oxazoline.[50] Several variations were synthesized with chiral and non-chiral oxazolines, but only initiators prepared from enantiopure **21** will be discussed here (Fig. 6). The zinc silylamide complex obtained with ligand **21** was obtained as diastereomers in a ratio of (R_{21},R_{Zn}):(R_{21},S_{Zn}) of 7:3. In this

case, the major diastereomer features a metal in the same configuration as the ligand, contrary to what was observed in the above-described previous system involving proligand **20**. The **21**-zinc-amido complex in the presence of isopropanol produced PLA of M_n up to 190 kg.mol^{-1}, Đ = 1.37, P_m = 0.87 with TOF of 3400 h^{-1}. No thermal properties were reported for this material. At lower temperature, a higher P_m is reached and the PLA showed a T_m of 188 ºC. Although the initiators were chiral, the isoselectivity was accounted for a CEC mechanism. The catalytic system even worked in the melt under immortal ROP conditions with a ratio $[LA]_0$:$[Zn]_0$:$[^iPrOH]_0$ of 20000:1:100 to produce isotactic PLA (P_m = 0.80) in a controlled manner. Unfortunately, no thermal analysis of the obtained polylactide was reported.

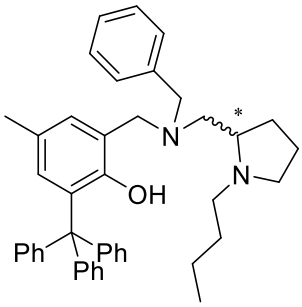

20a: (*S*)
20b: (*R*)

Ma, 2014

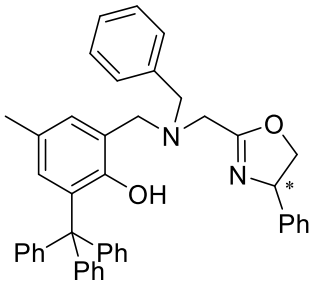

21a: (*R*)
21b: (*S*)

Wang and Ma, 2018

Fig. 7 Ligands developed for magnesium coordination

Using ligands **20a** and **20b**, Ma also reported the synthesis of magnesium derivatives (Fig. 7).[47] As in the case of the zinc catalysts, chiral-at-metal complexes were obtained. While zinc afforded a single diastereomer for a given ligand configuration, the magnesium complexes were obtained as a mixture of complexes (**20a**,R_{Mg}):(**20a**,S_{Mg}) and (**20b**,S_{Mg}):(**20b**,R_{Mg}) in a ratio of 7:1 respectively. Surprisingly, a selectivity switch from iso- to heterotacticity was observed when zinc was replaced by magnesium, under the same reaction conditions. The magnesium initiators produced heterotactic PLAs with P_r = 0.78 by CEC mechanism. The authors explained the difference in stereoselectivity by the formation of a hexa-coordinated magnesium complex during lactide ROP, compared to a penta-coordinated active site in the case of the zinc initiators. A detailed study on kinetics and coordination chemistry of the magnesium and zinc complexes (*e.g.*, addition of free ligand such as DMAP, coordinating or non-coordinating solvent (THF, toluene

and pyridine), variable temperature NMR experiments) supported this hypothesis. In 2018, Wang and Ma investigated aminophenol-oxazoline magnesium initiators for the isoselective ROP of lactide[51] similar to the zinc-based systems reported in 2017.[50] With ligands **21a** and **21b**, diastereomeric mixtures of magnesium complexes were formed in a ratio of 4:1 (Fig. 7). In the case of **21a**, namely the (*R*)-ligand, the main diastereomer is ($R_{\mathbf{22a}}$,R_{Mg}). In the case of **21b**, the ($S_{\mathbf{22b}}$,S_{Mg}) diastereomer is formed preferentially. This reflects the chemistry of the previously reported zinc complexes. The diastereomeric mixture of the amido complexes obtained with **21a** and **21b** formed after alcoholysis an isoselective initiator active for the ROP of *rac*-lactide in toluene. High molecular weight PLAs could be obtained in a controlled manner (M_n = 160 kg.mol^{-1}, $Đ$ ~ 1.5) with high activity (TOF = 22000 h^{-1}) at room temperature. The polylactides were moderately isotactic (P_m = 0.78) and no thermal properties were reported. The kinetics of ROPs were studied with *D*- and *L*-lactide and a 3.5-fold difference in polymerization rates tends to support an ESC mechanism. Moreover, the pseudo-first order kinetic plots for the reaction of *rac*-LA were clearly not linear and showed two polymerization rate constants associated with the ROP of the preferred and non-preferred lactide enantiomers. To further confirm an ESC mechanism, analysis of the PLA by ^{1}H homonuclear decoupling NMR showed that the tetrad ratio was such that [*rmr*] = [*mmr*] = [*rmm*] = [*mrm*]/2, in line with an ESC. In addition, the isotacticities of PLAs were higher at low and high lactide conversion and lower at ~ 50 % conversion. This is also characteristic of the formation of a tapered stereoblock polymer chain formed by ESC mechanism. It should be mentioned that since the ESC mechanism is clearly evidenced, both α and ESC statistics should have been used to describe the tacticity of the polymer instead of P_m and a CEC statistical model, at least for the latter polymers. Inspired by the work of Baker[52] and Coates[15,16] using the racemic mixture of Spassky's initiators,[35] the authors tested the potential of the racemic mixture of complexes containing mainly the ($R_{\mathbf{22a}}$,R_{Mg}) and ($S_{\mathbf{22b}}$,S_{Mg}) enantiomers. The ROP reaction was significantly faster and the PLA isotacticities increased. Remarkably, the racemic initiator mixture polymerized 5000 eq of *rac*-lactide in 5 minutes (TOF = 54000 h^{-1}) to produce with very high control, crystalline high molecular weight polylactides (M_n = 461 kg.mol^{-1}, $Đ$ = 1.26, P_m = 0.80, T_m = 164 ºC). In this case, ^{1}H homonuclear decoupling analyses of PLA revealed that the resulting PLAs are essentially stereoblocks as obtained by the CEC mechanism. As previously reported by Coates with aluminum initiators, the PLAs obtained here were essentially constituted of -*RRRRRRSSSSS*- sequences formed by a similar polymer chain exchange mechanism.

Additional studies confirmed the importance of ligand chirality and the dinuclear nature of the ROP active species.

2.4.3. Iron

Iron being a biocompatible, cheap and abundant metal, its use in catalysis has sparked considerable interest over the recent years. However very few examples of iron-initiated stereocontrolled ROP of lactide have been reported to date.[53,54,55]

In 2015, Byers reported an iron catalyst for the stereocontrolled ROP of *rac*- and *meso*-lactide.[54] The iron system is based on the well-known Brookhart iron catalyst for polymerization of olefins.[56] The iron (II) bisalkoxide complex with neutral ligand **22b** is a stable initiator giving better control over the ROP process compared to **22a** analog and those complexes were described as mono-initiating species even if the complexes possess two alkoxides (Fig. 8). Thus, the structure of the remaining non-initiating alkoxide in the complex is important as it can tune the steric and electronics of the initiator. ROP of *rac*-LA monomer with those achiral iron initiators produced moderately heterotactic enriched PLA with a P_r up to 0.75. The ROP of *meso*-LA with the achiral iron initiator gives a syndiotactic PLA as expected for a chain-end control process and as suggested by the stereocontrolled *rac*-LA ROP results. However, the analysis of the syndiotactic polylactides by ^{13}C NMR spectroscopy revealed an interesting tetrad distribution. This unexpected behavior was explained by the authors by the *in-situ* formation of a chiral tetradentate iron center in the complex during the ROP process by decoordination of one of the two imine arms giving a pro-(*R*) and a pro-(*S*) initiator after the first *meso*-lactide insertion. Thus, the formation of heterotactic PLA by ESC was explained by the epimerization of the chiral tetradentate iron center in the complex during the ROP process by a concerted coordination/decoordination of the two imine arms at the metal center after each *D*- or *L*-lactide insertion. The iron complexes showed original mechanistic features, but the polymerization control and catalytic performance of the iron complexes were rather limited ($1.3 < Đ < 1.6$, TOF < 10 h^{-1}). No thermal analysis of the syndiotactic PLA was reported.

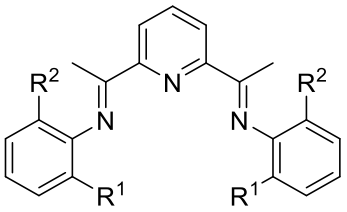

22a: $R^1 = R^2 = Me$
22b: $R^1 = H$, $R^2 = {}^tBu$

Byers, 2015

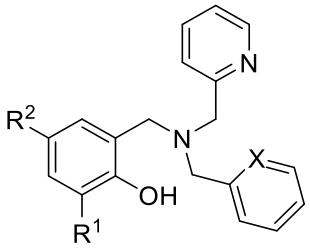

23a: X = N; $R^1 = C(Ph)_3$; $R^2 = Me$
23b: X = N; $R^1 = OMe$; $R^2 = Me$
23c: X = N; $R^1 = {}^iPr$; $R^2 = H$
23d: X = N; $R^1 = {}^{sec}Bu$; $R^2 = H$
23e: X = CH; $R^1 = C(Ph)_3$; $R^2 = Me$

Venditto and Thomas, 2019

Fig. 8 Examples of ligands used for iron complexation

Thomas, Venditto et al. reported a new series of iron complexes supported by readily available tripodal ligands **23a-e** and studied the influence of the ligand substituents on the microstructures of the produced PLAs (Fig. 8).[55] Bulky groups were chosen as the *ortho*-phenolate substituent to favor mononuclear complex formation and to increase the influence of the stereogenic center of the last inserted monomer, which controls the stereochemistry of propagation in these achiral iron initiators. Polymerization results indicated that, when the steric hindrance is sufficient, the *ortho*-substituents on the ligand do not significantly further influence the ability of the initiator to control monomer enchainment; for instance, changing the ligand *ortho*-substituents from trityl (**23a**) to *sec*-butyl (**23d**) groups resulted in virtually no change in isotacticity (P_m = 0.83, Scheme 2). However, by substituting a tetradentate ligand with a tridentate ligand (**23e**), the authors demonstrated a decrease in the stereoselectivity of the polymerization (P_m = 0.68). This influence may be due to the vacant coordination site, which leads to an additional monomer addition site and consequently affects the catalyst selectivity. Moreover, the iron initiators showed remarkable activities under mild conditions (TOF up to 32000 h^{-1}). The high P_m (0.83) for the PLA obtained with **23a** as ligand could be increased to 0.91 when performing the polymerization of 0 ºC (Scheme 2). For instance, a crystalline high molecular weight PLA having M_n = 52 kg.mol^{-1}, $Đ$ = 1.14, P_m = 0.82, T_m = 152 ºC, ΔH_m = 21 J.g^{-1} could be prepared in one minute. The stereoblock PLA were analyzed by wide-angle X-ray diffraction (WAXD), DSC, TGA and demonstrated to be obtained as thermally stable and industrially relevant stereocomplexes with high degradation

temperature offering a wide process temperature range. Later, the same team reported the Co and Zn analogs.[57]

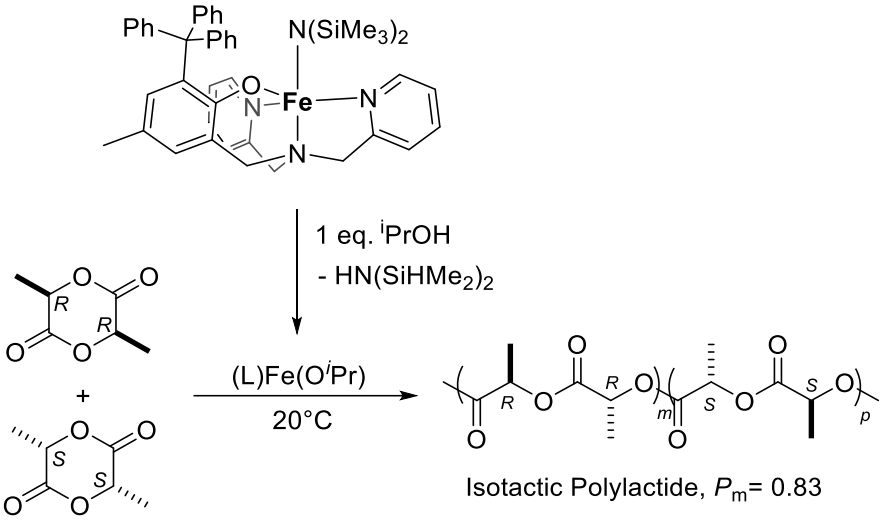

Scheme 2. Generation of an iron-based initiator for *i*-PLA synthesis

Although the Zn derivatives showed excellent rates (turnover frequency values up to 19500 h^{-1}) and high degrees of polymerization control, these complexes were not found to be as stereoselective as their iron counterparts (P_m up to 0.74), which further emphasizes the benefits of resorting to iron-based initiators. However, an interesting selectivity switch was observed with the corresponding Co complexes (P_r=0.61). Thus, the choice of metal center proved crucial in determining the level and mode of stereocontrol.

2.4.4. Rare-earth metals

After the discovery of the first yttrium-based stereoselective systems in the 2000s,[58] Williams reported yttrium initiators bearing achiral phosphosalen ligands **24** able to produce isotactic PLA.[59] The isotacticity of the obtained PLA was similar to Arnold's systems but with much lower activities (TOF > 100 h^{-1}) at –15 ºC. However, the polymerization is better controlled as the PLA formed exhibited the expected molecular weight based on the used monomer:initiator ratio. The highest isotacticities were obtained with **24a** as ligand. Interestingly, modifying the phosphosalen bridge in ligands **24a** and **24b**, for instance, switched the stereoselectivity of the yttrium catalyst to heterotactic preferences. High heterotacticities (P_r = 0.90) were achieved at room temperature with very high activities (TOF > 20000 h^{-1}).[60] Williams also reported in 2014 a study on the influence of the nature of the metal center on the stereochemical outcome in ROP of *rac*-

LA using the same proligand system. **24a** was coordinated to lutetium and lanthanide and compared to the previously reported yttrium analog (Fig. 9).[61] Lutetium affords isotactic PLA with low activity compared to the lanthanum analogs. Higher isotacticities are obtained with lutetium compared to yttrium (P_m = 0.80 versus P_m = 0.75 at room temperature, respectively) but with lower polymerization rates. However, the lanthanum initiator produces heterotactic PLAs. Such contrasted behaviors were explained by a more sterically congested metal coordination sphere with reduced fluxionality of the phosphorus substituents in the case of yttrium and lutetium. In contrast, a more open coordination geometry and fluxionality of the phosphorus substituents accounted for the heteroselectivity in the case of a larger metal center such as lanthanum.

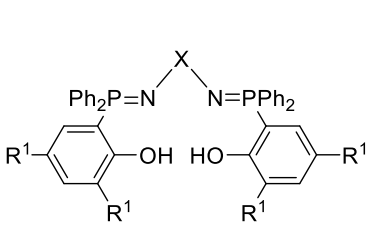

24a: X = -$(CH_2)_2$-NH-$(CH_2)_2$-; R^1 = ^{t}Bu
24b: X = -$(CH_2)_2$-; R^1 = ^{t}Bu
24c: X = -$(CH_2)_2$-; R^1 = $C(CH_3)_2Ph$

Williams, 2012, 2014 and 2017

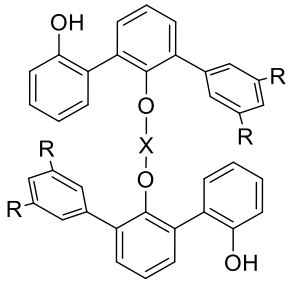

25a: X = -$(CH_2)_3$- ; R = ^{t}Bu
25b: X = -$(CH_2)_4$- ; R = ^{t}Bu
25c: X = -$(CH_2)_3$- ; R = H
25d: X = -$(CH_2)_4$- ; R = H

Xu, 2017

Fig. 9 Proligands used for rare-earth metals complexation

In 2017, Xu reported an isoselective yttrium initiator based on an bisphenol-bisether ligand system (O,O,O,O). By CEC mechanism, PLAs with P_m up to 0.90 were obtained at –15 ºC with the bulkier ligand system **25a** (Fig. 9). At room temperature, P_m up to 0.84 were obtained with **25a-b** with TOF > 2000 h^{-1}. T_m around 175 ºC were reported for those PLAs.[62]

2.4.5. Indium

In 2017, a new phosphosalen indium initiator featuring proligand **24c** was reported, producing highly isotactic PLA by ROP of *rac*-lactide.[63] For comparison, yttrium systems based on **24b-c** afforded heterotactic PLAs. Using the less bulky proligands **24b**, lower isotacticities were achieved. With **24c** as a ligand, alkoxide indium initiators produced highly isotactic PLAs (P_m = 0.87, T_m = 165 ºC) with reasonable activity (TOF ~ 500 h^{-1}). The ROP was well-controlled and high molecular weight PLAs

could be obtained (M_n up to 70 kg.mol^{-1}). As expected, ROP at lower temperature increased the isotacticities to P_m = 0.92 and the melting temperature of PLA increased to 179 ºC. A CEC mechanism was evidenced for the achiral indium initiators.

2.4.6. Group 4 (Ti, Zr, Hf)

Kol recently described group 4 metal-based initiators for the isoselective ROP of *rac*-lactide.[64] A series of salalen type of ligands were studied with different substitution patterns on the aromatic rings. Proligands **26a** and **26b** bearing halogen substituents in R^1 and R^2 position and the bulkiest substituent adamantyl (Ad) at the R^3 position formed the most isoselective initiators for zirconium and hafnium (Fig. 10). The activity of the initiators was modest at 70 ºC (TOF < 100) and the dispersity of the polymer slightly broadened ($Đ$ ~ 1.4). At this temperature, isotacticites of 0.82 < P_m < 0.89 could be obtained with both ligands either with hafnium or zirconium, the latter showing slightly higher isotacticities. These PLAs showed a T_m up to 180ºC with a high ΔH_m up to 65 J.g^{-1}, confirming the high crystallinity of PLAs. In the second DSC heating cycle, cold crystallization phenomena and a melting endotherm were also observed for the highly isotactic polylactides. Moreover, highly crystalline high molecular weight PLAs (up to 150 kg.mol^{-1}) were obtained.

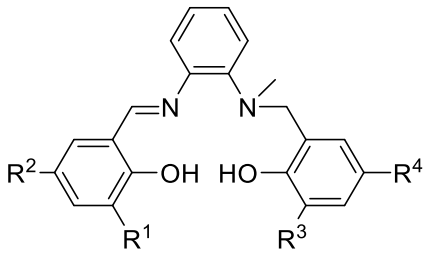

26a: R^1 = R^2 = Cl; R^3 = Ad; R^4 = Me
26b: R^1 = R^2 = Br; R^3 = Ad; R^4 = Me

Kol, 2017

Fig. 10 Proligands used for coordination on group 4 metals

In 2014, Jones reported the coordination of proligands **15c-e** (Fig. 5) on zirconium to form bis-isopropoxide complexes.[65] The enantiopure (*R,R*), the (*S,S*) and *meso*-configurations of the ligand were prepared. Moderately isotactic PLAs could be synthesized from the ROP in the molten monomer, with the enantiopure versions giving slightly higher isotaticties compared to the *meso* one (P_m = 0.70 *vs.* 0.66). However, at

room temperature, the *meso-(***15e**)Zr(O^{i}Pr)$_2$ produced highly isotactic materials with P_m up to 0.86 and higher polymerization rates. Upon coordination, the enantiopure C_2 symmetric ligands (*R*,*R*)-**15c** and (*S*,*S*)-**15d** formed "locked" single enantiomers of Δ and Λ zirconium complexes. These complexes exhibited a selectivity factor of 4 for the ROP of lactide enantiomers and are believed to exert stereocontrol via ESC mechanism. However, Jones demonstrated that the *meso*-**15e**, a C_s symmetric ligand afforded a fluxional zirconium complex upon coordination, where both Δ– and Λ-helix enantiomers coexist in a racemic mixture. Thus, the high isotacticity of the PLA obtained with the *meso*-complex was attributed to the helical switch between the Δ– and Λ-form depending on the lactide enantiomer inserted, producing an isotactic stereoblock PLA by a CEC mechanism.

With the same ligand system **15**, Jones reported later the influence of the metal center nature on the stereochemical outcome in the ROP of *rac*-lactide similarly to Williams's work. As mentioned previously with aluminum and zirconium, the *meso*-**15e** gave the highest stereoselectivities. Jones observed that the titanium-derived *meso*-initiator produced atactic PLAs, whereas the hafnium counterpart produced highly isotactic PLAs and the aluminum derivative was heteroselective. The hafnium initiators could produce isotactic PLAs even under bulk ROP conditions (130 ºC), though the P_m was rather modest (P_m = 0.7). ROP in toluene at 50 ºC afford crystalline PLA with high melting temperature (181 ºC) for a calculated P_m of 0.84. The hafnium system was more isoselective than the zirconium analog under the same conditions (P_m = 0.80 *vs.* 0.75 at 70 ºC in toluene). On the contrary to Williams's observation, the larger hafnium gave isotactic polymers and the smaller aluminum atom is heteroselective. Coordination number and geometry in the complexes were proposed to account for these observations.

2.4.7. Copper

Copper complexes were initially investigated to replace stannous octanoate in bulk polymerizations and their catalytic activities were usually modest. Despite the increasing number of studies dealing with the ROP of *rac*-lactide using copper complexes for the last decade, there is still a limited number of such initiators capable of producing heterotactic- or isotactic-enriched PLA. Schaper described the first stereocontrolled ROP of *rac*-lactide using copper complexes.[66] Chiral diiminopyrrole copper complexes featuring **26** proligands showed a preference for isotactic chain growth in *rac*-lactide polymerization (Fig. 11).[66a] However, the P_m value of the PLA obtained is modest (P_m =

0.7) and the activity of is rather moderate (TOF < 20 h^{-1}). The dinuclear nature of the active species played an important role in dictating the stereocontrol and thus, the bridging ligand is crucial for the stereocontrol. The chirality of the ligand does not affect the stereocontrol and the stereocontrol mechanism was confirmed to be a chain-end control. Unfortunately, despite numerous structural variations of ligands and ligand substitution patterns (as in **27a-e**), no improvement on stereoselectivity could be achieved.[66b,c]

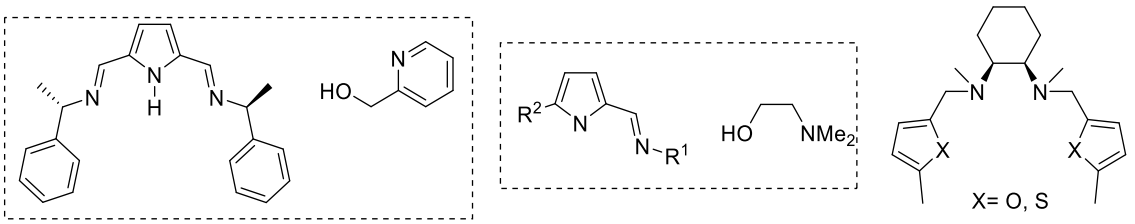

26

Schaper, 2015

27a: R^1 = Naphtyl; R^2 = HC=N-R^1
27b: R^1 = 2,6-$(CH_3)_2C_4H_3$; R^2 = HC=N-R^1
27c: R^1 = cyclohexyl; R^2 = HC=N-R^1
27d: R^1 = $CH(Ph)_2$; R^2 = HC=N-R^1
27e: R^1 = (*S*)-$CH(CH_3)Ph$; R^2 = Me

Schaper, 2017

28

Jeong, 2018

Fig. 11 Proligand systems developed for copper coordination

Jeong also reported high activities with diamino copper catalysts formed *in situ* from the respective copper chloride complex derived from ligand **28** and lithium alkoxide. These chiral derivatives featured high activities and selectivities, affording highly heterotactic PLA (P_r up to 0.90) from *rac*-LA, by incorporating the (*R*,*R*)- and (*S*,*S*)-LA in an alternating fashion (Fig. 11).[67]

3. Stereocontrolled ROP of lactones

The vast majority of advances in stereoselective ring opening polymerization of lactones focused on the ROP of strained β-lactone derivatives, substituted in 3-position, which afforded the corresponding polyhydroxyalkanoates. Additional examples consisted of ROP of various chiral lactones.

Rare-earth metals systems held the lion's share in this specific field, with yttrium being the more frequently used element, owing mostly to their high Lewis acidity and ability to accommodate stereoenforcing multidentate ligands. These predominantly featured two phenoxide moieties, along with two donor centers, such as [O^-,*N*,*O*,O^-] bisphenoxyaminoalkoxy, or [O^-,*N*,*N*,O^-] with various topologies and *N*-based ligand

moieties, such as bisphenoxybisamino (**29**), *salan* (**30**) or *salen* (**31**) (Fig. 12). These imposed a rather rigid coordination sphere around the metal. Tuning their steric and electronic features resulted in a tailored propagating center able to convey, in some instances, remarkable degrees of control over the stereoselective ROP of non-symmetrical lactones. As will be exemplified, this control was highly dependent on the structure of the considered monomer: whereas bisphenoxyamino-donor ligands may appear to be privileged pro-ligands at first glance, it must be taken into account that this owes much to the possibility to fine-tuning their structure, as high stereoselectivity derives from the characteristics of the phenolate moieties substituents, whether steric or electronic features, or from the nature of the fourth donor function (X on Fig. 12). In the next sections, we will review main advances since the 2010s in the stereocontrolled ROP of *β*-butyrolactone (BBL), followed by some of its functionalized analogues, and finally of additional examples of monomers.

To briefly remind the reader about the basis behind the recent works, the first striking results in the syndiospecific polymerization of BBL into P3HB were achieved in 2006, using an yttrium alkoxide derivative supported by a [O^-,*N*,*O*,O^-] bisphenoxyaminoalkoxy ligand (**29,** Fig. 12).[68] With the cumyl group as the *ortho*-substituent on the phenolate moieties (**29b**), a probability of racemic linkages between monomer units (P_r) as high as 0.94 was achieved, while the use of the *t*-butyl analogue (**29a**) resulted in a lower efficiency in stereocontrol. The resulting polymers feature M_n up to 50 kg mol^{-1}, narrow mass distribution ($Đ$ = 1.03- 1.18) and melting temperature up to 178 °C. These results sparked intense exploitation of this class of catalysts, as will be described below. The impact of ligand modification on the resulting polymer was probed by the same authors: A series of 5 amino-alkoxybisphenolate ligand frameworks with varying steric and electronic features (type **29**, Fig. 12) complexed onto yttrium silylamide were assessed in the ROP of racemic lactide and BBL.[69] Regarding BBL, from which syndiotactic PHBs are obtained, the probability for racemic linkages between monomer units was strongly dependent on the nature of the *ortho* substituent on the phenolate moieties. The most efficient systems combined bulk and presence of aromatic ring(s), with trityl groups (**29c**, Fig. 12) conveying the highest syndioselectivity (P_r = 0.95). DFT computational analysis on model intermediates revealed the existence of stabilizing interactions between a hydrogen from a methylene group within the ring-opened lactone and the π-system of an aromatic group of a phenolate *ortho* substituent.

The importance of this phenomenon in the catalytic cycle, and most precisely, as a syndioselectivity-orienting factor, has yet to be demonstrated by further DFT studies.

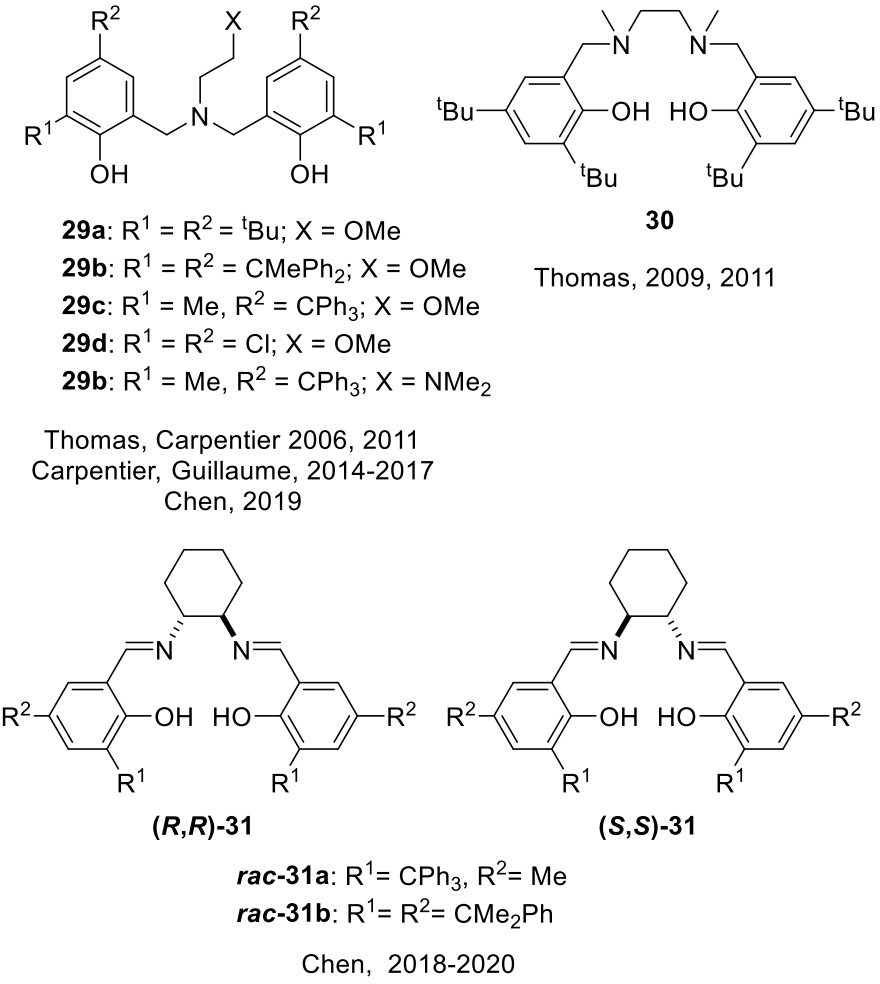

Fig. 12 Ligand scaffolds used in lactone ROP initiators design

Thomas and coworkers expanded the scope of ligand scaffolds able to convey efficient stereocontrol. The authors reported the expeditious synthesis of yttrium alkoxides bearing the salan ligand **30** (Fig. 12) and their use for the ROP of BBL.[70] This system afforded highly syndiotactic PHBs, with a P_r value of 0.90, and with good control of the mass distribution. Detailed DFT investigations on the stereoselectivity of the first two monomers insertion are fully consistent with the experimentally observed tacticity, which originates from a CEC (Fig. 13).

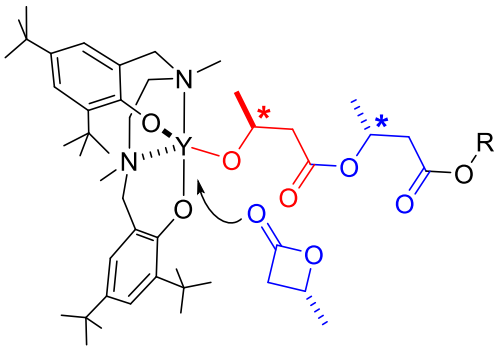

Fig. 13 Representation of the geometry of the yttrium-salan initiator **30**-**Y**

In contrast to catalytic systems leading to syndiotactic PHB, those affording isotactic PHB are much less common. This was addressed in an alternative organometallic approach to stereoselective ROP of BBL, namely the use of supported catalysts prepared via a surface organometallic approach (Fig. 14).[71] Indeed, well-defined silica-grafted neodymium borohydride species initiated the ROP of BBL into isoenriched PHB, with P_m of 0.85, and dispersity of 1.18. The low PDI is consistent with a unique type of propagating center, as expected from the controlled synthetic procedure along with the characterization data. Although these results were achieved using highly dehydrated silica as inorganic carrier, the influence of the support dehydration (and thus, the distribution and nature of initiating sites) on the catalytic performance of the materials was probed with amido-based initiators.[72] The isotacticity of the resulting PHBs could be modulated from P_r = 0.70 to P_r = 0.80 by adjusting the preparative procedures (dehydration of silica at 200 and 700 °C, respectively). Questions remain pending concerning the mode of stereocontrol.[73]

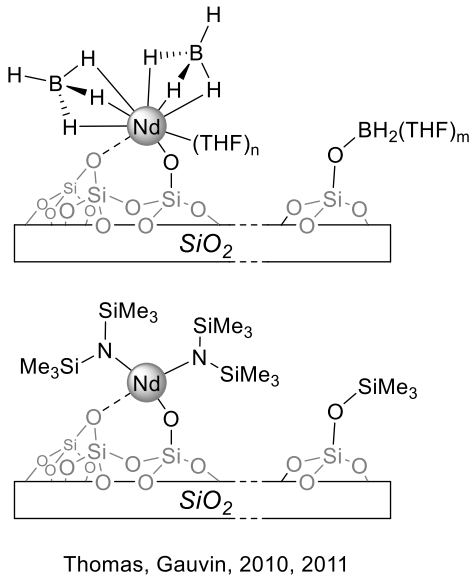

Thomas, Gauvin, 2010, 2011

Fig. 14 Isoselective supported Nd-based initiators

A recent breakthrough in the synthesis of isotactic P3HB was achieved by Chen when exploring the pathways to this polymer. The use of methyl-substituted *rac*-diolide (DL^{Me}) as an alternative monomer to BBL was proposed, by establishing a connection with the fact that cyclic dimer of lactic acid (lactide) allows efficient production of PLA (Scheme 3).[74] In this case, the best initiators proved to be chiral yttrium salen species, featuring bulky substituents at the phenoxide *ortho* position (**31a**, Fig. 12). These complexes featured remarkable catalytic properties: They induced the formation of pure isotactic PHB (P_m>99%), with excellent mass control ($Đ$ < 1.07 for up to 1200 monomer equivalents per initiator) and high productivity.

No significant results were obtained with the same system when applied in the ROP of BBL, demonstrating that the design of efficient, selective initiating systems is highly dependent on the addressed monomer. On the other hand, the use of tetradentate ligands yttrium complexes based on **29** (Fig. 12) known to be efficient in ROP of BBL resulted in modest results. Mechanistic studies as well as ^{13}C NMR microstructure analysis showed that ESC is responsible for the polymer tacticity. Moreover, the high stereoselectivity allowed efficient kinetic resolution to take place when using enantiomerically pure initiators, with a stereoselectivity factor *s* being over 10^3. Thus, the use of the racemic catalyst (composed of equimolar (*R*,*R*) and (*S*,*S*) isomers) towards *rac*-DL^{Me} afforded a mixture of enantiomerically pure P3HB chains. Similarly, the (*R*,*R*) initiator reacted with *rac*-DL^{Me} to afford 50% conversion into poly[(*S*,*S*)-DL^{Me}], leaving unreacted (*R*,*R*)-DL^{Me}. The thermal properties of enantiomerically pure P3HB were

investigated: T_m up to 175 °C were observed, nearly identical to those of the commercial natural poly [(*R*)-3HB]. Interestingly, the synthetic polymers featured molecular mass up to $1.54.10^5$ g.mol with a polydispersity of 1.01, compared to that of their natural counterparts of about 2.0 as produced from bacteria. MALDI-TOF investigations indicated that the polymers were linear when using a high monomer/initiator ratio, while transesterification side-reactions occurred at low monomer ratio. In subsequent studies, kinetic and stereocontrol mechanism aspects for this system were investigated.[75] The rate law for the ROP of *rac*-DL mediated by this catalytic system was determined, showing a 1st order in both the monomer and the catalyst. DFT calculations confirmed that the operating stereo-inducing mechanism was of the ESC type, as the energetics favored the consecutive insertion of the same DL^{Me} stereoisomer from the *rac* mixture.

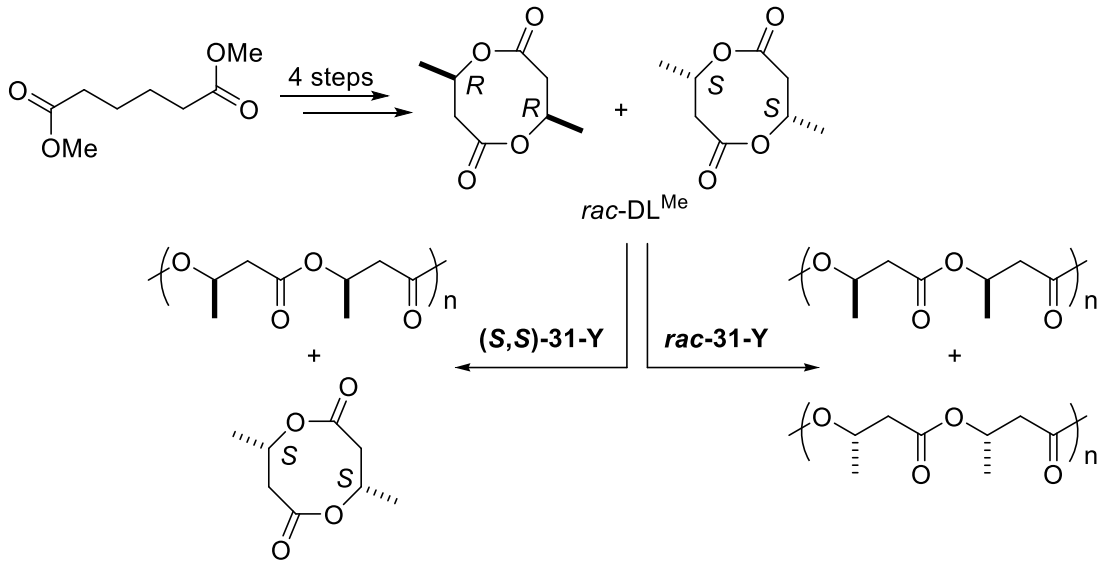

Scheme 3. Preparation and ROP of diolides

This approach was extended to further members of the diolide family. Indeed, in addition to methyl-substituted monomers, the *rac* ethyl and butyl derivatives (*rac*-DL^{Et} and *rac*-DL^{Bu}, respectively) were also polymerized using similar catalytic systems. In such cases, the optimal system was based on ligand **31b** (Fig. 12), combining high activity and isoselectivity (P_m = 0.96 and 0.97 from *rac*-DL^{Et} and *rac*-DL^{Bu}, respectively). Random copolymers were produced using the yttrium-**31b** initiator, with a preference for *rac*-DL^{Me} insertion over that of *rac*-DL^{Et} or *rac*-DL^{Bu}. For both copolymers, a good to excellent mass control was achieved, while high molar weights could be reached (over 10^5 $g.mol^{-1}$). Thermal and mechanical properties were investigated, demonstrating that

the incorporation of monomers with longer alkyl side chain decreases the melting temperature, and that the copolymers behave similarly to polyolefins such as polyethylene and isotactic polypropylene when considering their tensile strength, Young's modulus and elongation at break.

As the synthesis of the diolide monomers from dimethyl succinate is rather tedious and involves formation of the *meso* stereoisomers, the latter were also taken advantage of by incorporation in the preparation of stereosequenced polyhydroxyalkanoates.[76] It was shown that *meso*-DL is stereoselectively ring-opened into syndiotactic P3HB by Y and La derivatives of the salen ligand **31a**, with the yttrium species being more active than its lanthanum counterpart, albeit at the expense of syndiotacticity (P_r = 0.81 for Y *vs.* 0.92 for La). In competition studies, *meso*-DL^{Me} proved less reactive than *rac*-DL^{Me}, with a ratio of reaction rates of about 80 in favor of *rac*-DL^{Me}. Thus, using a stoichiometric mixture of *meso*- and *rac*-DL^{Me}, a stereodiblock structure was obtained. Specifically, the authors proposed, based on comparative studies, that the isotactic and syndiotactic blocks are linked by intermediate sections comprising both stereoisomers, resulting in a tapered stereodiblock copolymer. *Inter alia*, evidence was provided by comparison with the thermal properties of the pure stereodiblock copolymer prepared by the consecutive addition of *rac*- and *meso*-DL^{Me}. Interesting mechanical properties were obtained with these new polyesters, such as for instance a 6-fold increase in ductility when compared to isotactic P3HB. Further tuning of the thermal and mechanical properties of this family of copolymers was achieved by playing on the differences in relative reaction rates between *meso*- and *rac*-stereoisomers of DL^{Me} and DL^{Et}.

Interestingly, the remarkable efficiency of the yttrium salan scaffold **30** regarding the monomer discrimination was implemented in a conceptually new copolymerization, involving two different enantiopure 3-alkyl-β-lactones of opposite configuration.[77] The resulting copolymers thus consisted of alternation of the two lactone monomers (with a percentage of alternation ranging from 90% to 94%), while featuring high molecular mass and low polydispersity (from 1.10 to 1.49). This concept was put to use in related studies on functionalized monomers, as will be briefly mentioned below. Further efforts were devoted to the stereoselective polymerization of alternative monomers, derived from 3-functionalized β-butyrolactones or other monomers. The efficient stereocontrol from the [O^-,*N*,*O*,O^-] and [O^-,*N*,*N*,O^-] yttrium systems was instrumental in these examples. As

illustrated below, thanks to the facile ligand tuning, contrasting features emerged regarding the tuning of the ROP stereoselectivity.

A stereoselective ROP approach was harnessed to access a specific class of poly(hydroxyalkanaote)s, namely poly(β-malic acid) derivatives (PMLA) using alkyl-β-malolactonates (MLA^R) monomers (Scheme 4). The latter ring-opened into the corresponding $PMLA^R$ with good to high probability of *r* enchainments, from 0.68 to over 0.95.[78] The best system in terms of stereocontrol (P_r>0.95) was based on the chloro-substituted ligand scaffold **29d**. This contrasts with previous observations made with BBL, where the most efficient systems featured bulky alkyl substituents, while polymerization with **29d** is almost aspecific. Thus, two examples of syndiotactic $PMLA^R$ were prepared, constituting the first examples of this class of materials, so far inaccessible by classical methods. The microstructure analysis was in line with a CEC mechanism. However, the high syndioselectivity came along with moderate control over molar mass distribution, the polydispersity being higher than 1.54. Based on a previously established concept,[77] the use of two different enantiopure $PMLA^R$ of opposite configuration led to the formation of an alternating copolymer, with the percentage of alternation being over 95% for the most selective, **29d**-based system. The structure was probed by ^{13}C NMR along with MALDI-TOF and ESI MS-MS studies. An example of post-polymerization reactivity was given, as treatment under hydrogen in the presence of a heterogeneous Pd catalyst afforded an original alternating copolymer.

In a follow-up study, performed on a set of three MLA^R monomers (R= allyl, benzyl and methyl), the CEC mechanism was further probed by ^{13}C NMR microstructure analysis, combined with statistical models on tetrads' relative contributions.[79] Thus, it was proposed that the syndioselectivity in the ROP of MLA^{All} and MLA^{Bn} originated from a first-order Markov mechanism: The selectivity for the addition of a new monomer to the growing chain is influenced only by the configuration of the last monomeric unit. The case of ROP of MLA^{Me} was distinct: Statistical analysis was more in line with a second-order Markov mechanism, where the addition of a new monomer is influenced by the configuration of both the last and penultimate monomeric units within the polyester chain. Beyond these observations, the origin of the higher efficiency of the halide-substituted ligand in terms of stereocontrol remained elusive. Preliminary DFT investigations ruled out the occurrence of halogen bonding within the potential

intermediates. The actual mechanism was not probed yet, and the origin of stereoinduction remains to be determined.

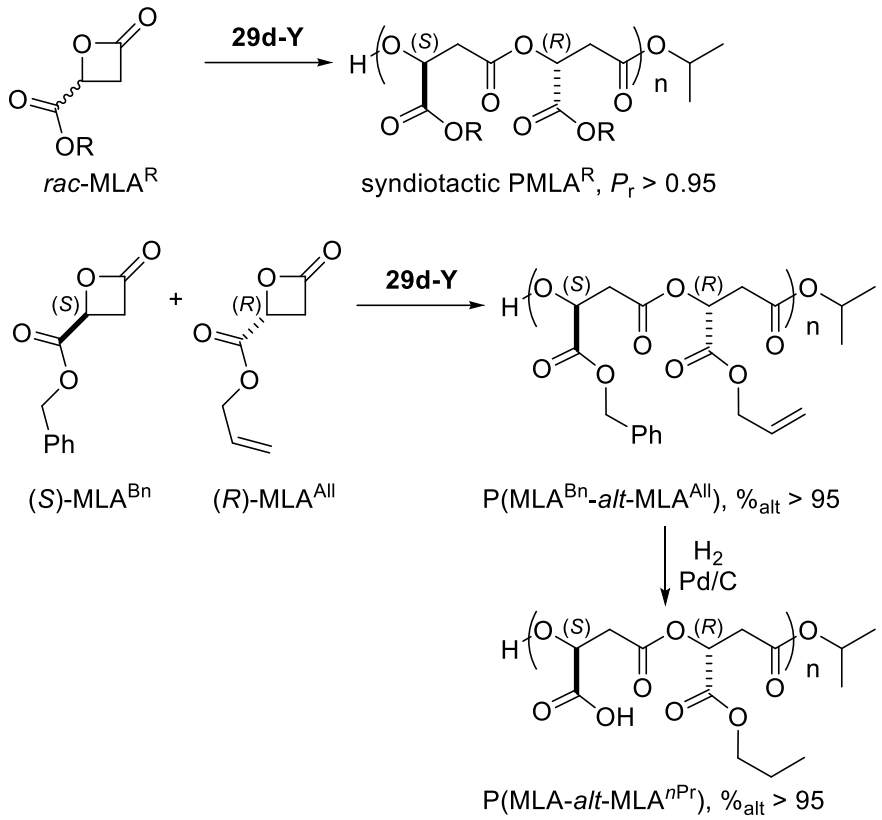

Scheme 4. ROP of alkyl-β-malolactonates (MLA^R) into poly(β-malic acid) derivatives (PMLA)

The ROP of functionalized β-lactones such 4-alkoxy methylene β-propiolactones (BPL) led to the interesting observation of a selectivity change from syndio- to isoselective polymerization, when switching from alkyl- to chloro- substitution in [O^-,*N*,*X*,O^-] tetradentate donor-aminobisphenolate ligands complexed onto yttrium (Scheme 5).[80] Thus, the **29b** yttrium-based initiator led to P_r values of up to 0.91, while **29d** bearing an *ortho*-chloride substituent on the phenolate moieties afforded P_r of 0.07 (Fig. 12). The nature of the donor functionality on the ligand framework mostly influenced the activity, with NMe_2 leading to higher productivity than OMe. ^{13}C NMR studies indicated that the stereoselectivity stems from CEC. Based on DFT studies, the change in selectivity was proposed to arise from specific interactions between the chloride and the OCH_2 groups from the alkoxy moiety within the growing polymer chains, which kinetically favors the consecutive insertion of monomers with identical configuration, thus leading to isotactic

chains. As a comparison, ester-substituted monomers MLA^R (where a methylene is formally replaced by a carbonyl moiety) ring-opened into syndiotactic polymers (*vide supra*) with the same chloride-substituted initiator, illustrating the elusiveness of a general predictive approach.

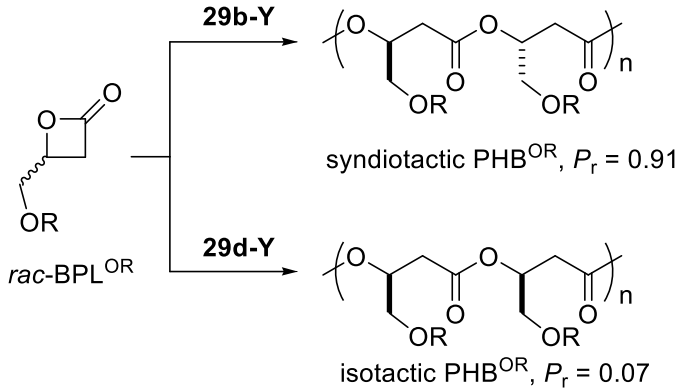

Scheme 5. ROP of 4-alkoxy methylene β-propiolactones (BPL) into functionalized PHBs

As a final salient example on stereoselective ring-opening polymerization of unsymmetrical lactones, Chen demonstrated the interest of exploring different catalyst architectures when addressing the ROP of monomers such as *trans*-cyclohexyl-ring-fused γ-butyrolactone (CBL, Scheme 6).[81] It was used as a mixture of the (*R*,*R*) and (*S*,*S*) isomers, designated as *rac*-CBL. Screening of various catalysts ended up in identifying yttrium complexes bearing tetradentate [O^-,*N*,*X*,O^-] ligands. The nature of the X moiety within the ligand's side-arm was shown to govern the selectivity of the ROP process. Indeed, the use of OMe- functionalized ligand **29a** (Fig. 12) afforded a moderately heterotactic polyester (resulting from consecutive insertions of monomers of opposite configuration) with P_r of about 0.75 under optimized conditions. On the other hand, with a NMe_2-functionalized ligand bearing bulky *ortho*-substituents on the phenoxide moieties such as **29e** (Scheme 6), a highly isotactic PCBL could be produced with P_m up to 0.95 (T_m = 171 °C). In both cases, low temperatures were key in achieving high selectivity. Microstructure analysis by ^{13}C NMR showed that selectivity stems from CEC. MALDI-TOF investigations established the linear structure of the polyesters produced. A further interesting point of this study was the formation of a stereocomplex between the blocks of *R*- and *S*- units within the isotactic PCBL formed, thus providing superior thermal performance compared to the pure isotactic polymer. Recyclability studies demonstrated that the pure monomer could be formed upon heating in the presence of zinc chloride, thus closing a loop linking the monomer and the corresponding polyester.

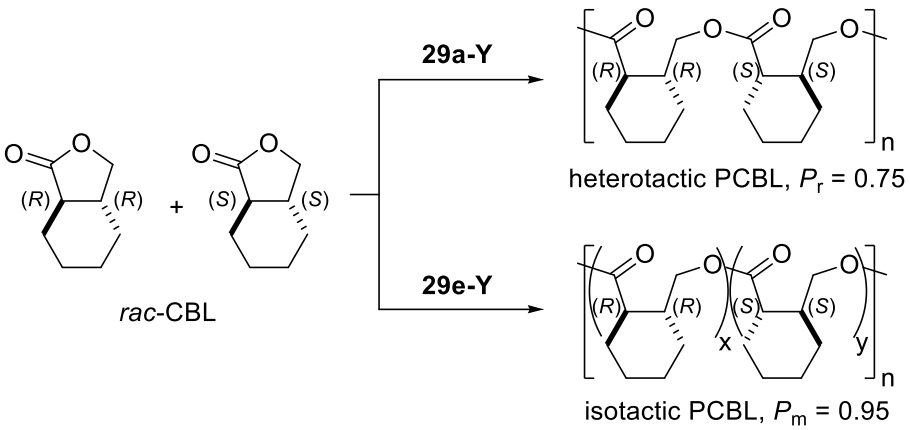

Scheme 6. ROP of *trans*-cyclohexyl-ring-fused γ-butyrolactone (CBL).

The possibilities opened by lactones copolymerization in terms of materials properties modulation were recently explored by Thomas, Venditto *et al.*[82] Taking advantage of the remarkable reactivity of (salan)Y(III) complexes (**30-Y**), they reported an efficient route for the ring-opening copolymerization of *β*-butyrolactone (BBL) with *ε*-decalactone (*ε*-DL). By this way, several di- and triblock copolymers were successfully synthesized by sequential addition of the monomers (Scheme 7). The microstructure of the corresponding block copolymers revealed the presence of syndiotactic poly(3-hydroxybutyrate) blocks. The authors demonstrated that the PHB blocks were able to crystallize even in the presence of long amorphous PDL blocks. It was also observed that the microphase separation of the PDL-*b*-PHB copolymers into PHB and PDL rich domains had an impact on the glass transition temperature of both blocks. Finally, the physical behavior of these copolymers (*e.g.*, flexibility/stiffness) could be tuned by changing the *ε*-DL/BBL ratio, due to the presence of a highly flexible phase associated with a rigid crystalline phase. Such physical behavior makes these copolymers industrially interesting, while illustrating the potential of the ROP approach in the design of advanced materials.

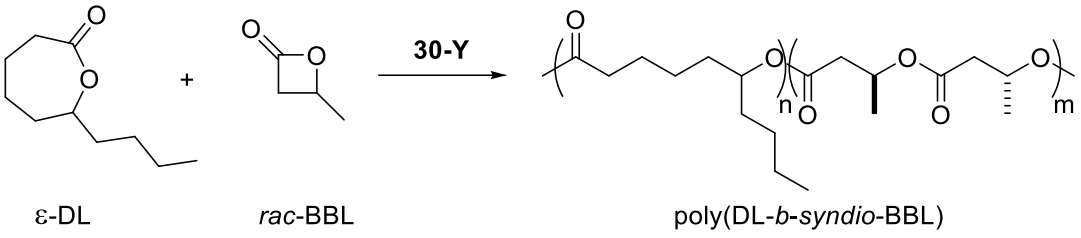

Scheme 7. Synthesis of block copolymers from ε-DL and *rac*-BBL

4. Stereocontrolled ROP of *O*-carboxyanhydrides

Aliphatic polyesters such as PLA may be prepared by the ring-opening polymerization of cyclic esters (*vide supra*).[12a] However, this route restricts the polymer architectures to those of the cyclic esters that are available. In particular, there is a lack of side-chain functionality in the monomers involved. A different approach, the ring-opening copolymerization of epoxides and cyclic anhydrides, has the potential to produce a wider variety of polymer backbone structures through a higher accessibility of the heterocyclic monomers.[6,83,84] In that case, stereoselective synthesis of polyesters with pendant side-chain functional groups remains challenging. In this regard, the ROP of 1,3-dioxolane-2,4-diones, so-called *O*-carboxyanhydrides (OCAs), can give diverse aliphatic polyesters with different functional groups because of easy modification of the side group of OCAs. Although the preparation of dioxolanedione monomers involves the use of highly toxic phosgene (or one of its derivatives)[85] by condensation with α-hydroxy acids, this method represents an interesting alternative to prepare stereoregular (co)polymers.

Tong recently described an approach that combines photoredox Ni/Ir catalysis with the use of a Zn-alkoxide for the ROP of (enantiomerically pure) OCAs, therefore affording isotactic polyesters with high molecular weights (M_n up to 140 kg.mol^{-1}) and narrow molecular weight distributions.[86] Mechanistic studies indicated that the role of a photoredox Ni/Ir system at low temperature (–20 °C) was to accelerate ring-opening and decarboxylation of the monomer for chain propagation. These authors also used a similar protocol to synthesize stereoblock polyesters, as well as gradient copolymers.[87]

In 2017, Wu and coworkers described the synthesis of syndiotactic homopolymers (P_r up to 0.95) from racemic OCAs using achiral zirconium and hafnium complexes bearing bulky aminotrisphenate ligands, presumably *via* a chain-end-control mechanism.[88] Inspired by previous findings,[77] these authors also performed the selective ROP of enantiomerically pure but different OCAs to obtain alternating copolymers of α-hydroxy acids. Tao and Wang recently reported a bifunctional organocatalyst containing a thiourea group and a pyridine moiety.[89] These organic catalysts were moisture-stable, recyclable, and easy to use, allowing selective ring-opening polymerization of OCAs without epimerization. In particular, it was shown that the close vicinity of both functional

groups in the same catalyst allows the use of mild bases, thereby limiting epimerization for polymerization.

5. Conclusion

In order to obtain stereoregular polyesters, catalyst design is a valid option. Over the past two decades, coordination polymerization using well-defined metal complexes has played a prominent role, but in recent years, the focus has been on the synthesis of organocatalysts that are active polymerization initiators for the ring-opening polymerization of lactide and β-butyrolactone to give poly(lactide) and poly(3-hydroxybutyrate), respectively. Most organocatalysts have the advantage of being water and air tolerant and provide polymers free of residual metal contaminants, which is attractive for some applications. However, these initiators generally exhibit high stereoselectivities but low catalytic activities and result in the formation of low molecular weight polyesters while operating in environmentally harmful solvents. In order to obtain more efficient organocatalysts, it will therefore be essential to define new targets to be achieved in future systems. Concerning organometallic systems, their activity and selectivity has become excellent. In a first instance, investigation of the coordination chemistry of the considered metal/(pro)ligand couple should be performed, as this process may not lead to a trivial outcome: In some cases, mixtures of initiating systems with contrasting stereoselective abilities may be obtained, depending on reaction conditions and selected organometallic precursors. This can also be complexified by phenomena specific to a given initiating system, such as the occurrence of exchanges of growing chains between metallic centers, or the formation of polynuclear entities with different stereodirecting capacity. These can lead to polymers featuring unconventional microstructure, a peculiarity which could be harnessed in the design of tailored materials provided that interesting properties could result from this, and that control over such processes can be enforced.

On the same line of thought, precise assessment of polymers' microstructure is a cornerstone in the development and understanding of efficient systems, as this gives information not only on the type of tacticity, but also on the propagation mechanism and potentially on the involvement of distinct propagating centers with distinct stereoselectivity ability. This implies that thorough examination of NMR features of

(co)polymers should accompany synthetic studies when discussing microstructures and aiming at properly describing the synthesized materials.

On the other hand, when aiming at the stereoselective polymerization of a given monomer, it is likely that the key elements for success are still identified by serendipity. This is well exemplified by the selectivity switch observed when comparing the switch in stereoselectivity when using two different metals complexed onto the same ligand, or when adjusting a ligand structure by rather limited modification. Nevertheless, tendencies are identified. Beyond the strong Lewis acidity and the rather crowded first coordination sphere required, an important factor for the design of efficient stereoselective initiating systems is the steric and/or electronic tuning within the second coordination sphere of the metal center. Yet, the weak stereodirecting interactions allowing successful stereocontrol were identified a posteriori, mainly from DFT calculations. It can be envisioned that in the future, theoretical calculations will play a more important role in finding effective initiator/monomer/polymer combinations.

In addition, polymerization reactions under homogeneous conditions result in contamination of the polymer with metal residues and loss of the catalyst. Therefore, supported heterogeneous catalysts can represent an attractive approach to cleaner process design and be expected to be very useful for the ROP of cyclic esters. Interestingly, immobilization of initiators onto inorganic supports has led to an increase in the stereoselectivity of the ROP process, demonstrating the ability of the surface to convey stereoselection, most probably via CEC mechanism. The development of this approach would however require the design of efficient separation of the supported species by allowing cleavage of the growing chain from the initiating center, for instance by using a chain transfer agent. The studies described in this review article demonstrate that the stereoselective synthesis of aliphatic polyesters is expected to yield new types of innovative materials for a wide range of applications. However, these materials have yet to become more cost-competitive with petroleum-based analogues through advances in synthetic methods and production processes.[90] In the authors' opinion, an increase in the market share of such plastics should ideally come from a decrease in the use of low-value, polluting petroleum-derived plastics and an increase in the number of applications of biodegradable materials derived from biomass. A possible solution could be the use of these polymers in combination with other types of materials to form (bio)composites. In this respect, plant fibers seem to be particularly promising materials. This should allow

the production of improved innovative materials with original properties that should open new horizons.

References

1 Data from European Bioplastics, https://www.european-bioplastics.org/bioplastics/materials/ accessed on 8 July 2021.

2 J. R. Jambeck, R. Geyer, C. Wilcox, T. R. Siegler, M. Perryman, A. Andrady, R. Narayan and K. L. Law, *Science*, 2015, **347**, 768−771.

3 (a) A. Gandini and T. M. Lacerda, *Prog. Polym. Sci*., 2015, **48**, 1−39; (b) M. J.-L. Tschan, E. Brulé, P. Haquette and C. M. Thomas, *Polym. Chem*., 2012, **3**, 836−851; (c) C. K. Williams and M. A. Hillmyer, *Polymer Rev*., 2008, **48**, 1−10; (d) Y. Zhu, C. Romain and C. K. Williams, *Nature*, 2016, **540**, 354−362; (e) X. Zhang, M. Fevre, G. O. Jones and R. M. Waymouth, *Chem. Rev*., 2017, **118**, 839−885.

4 (a) M. Hong and E. Y.-X. Chen, *Green Chem*., 2017, **19**, 3692-3706; (b) R. A. Gross and B. Kalra, *Science*, 2002, **297**, 803−807. (c) G. W. Coates and Y. D. Y. L. Getzler, *Nat. Rev. Mater*., 2020, **5**, 501–516.

5 O. Dechy-Cabaret, B. Martin-Vaca and D. Bourissou, *Chem. Rev.*, 2004, **104**, 6147-6176.

6 (a) R. C. Jeske, J. M. Rowley and G. W. Coates, *Angew. Chem., Int. Ed*., 2008, **47**, 6041-6044; (b) C. Robert, F. de Montigny and C. M. Thomas, *Nat. Commun*., 2011, **2**, 586; (c) J. M. Longo, M. J. Sanford and G. W. Coates, *Chem Rev*., 2016, **116**, 15167−15197; (d) S. Paul, Y. Zhu, C. Romain, R. Brooks, P. K. Saini and C. K. Williams, *Chem. Commun.*, 2015, **51**, 6459−6479.

7 (a) W. N. Ottou, H. Sardon, D. Mecerreyes, J. Vignolle and D. Taton, *Prog. Polym. Sci*., 2016, **56**, 64−115; (b) A. P. Dove, *ACS Macro Lett.*, 2012, **1**, 1409−1412; c) M. Ji, M. Wu, J. Han, F. Zhang, H. Peng and L. Guo, *Curr. Org. Chem.*, 2021, **25**, 272−286; (d) K. Nozaki and K. Fukushima, *Macromolecules*, 2020, **53**, 5018−5022; (e) A. Basterretxea, C. JEhanno, D. Mecerreyes and H. Sardon, *ACS Macro Lett*., 2019, **8**, 1055−1062; (f) C. Thomas and B. Bibal, *Green Chem*., 2014, **16**, 1687−1699.

8 J. C. Worsh, H. Prydderch, S. Jimaja, P. Bexis, M. L. Becker and A. P. Dove, *Nat. Rev. Chem.*, 2019, **3**, 514.

9 (a) J. Slager and A. J. Domb, *Adv. Drug. Del. Rev*., 2003, **55**, 549−583; (b) G.-P. Wu, S.-D. Jiang, X.-B. Lu, W.-M. Ren and S.-K. Yan, *Chin. J. Polym. Sci*., 2012, **30**, 487−492; (c) F. Auiemma, C. De Rosa, M. R. Di Caprio, R. Di Girolamo, W. C. Ellis and G. W. Coates, *Angew. Chem. Int. Ed*., 2015, **54**, 125−1218.

10 A. Le Borgne and N. Spassky, *Polymer*, 1989, **30**, 2312-2319.

11 M. I. Childers, J. M. Longo, N. J. van Zee, A. M. Lapointe and G. W Coates, *Chem. Rev.*, 2014, **114**, 8129−8152.

12 (a) C. M. Thomas, *Chem. Soc. Rev*., 2010, **39**, 165−; (b) M. J. Stanford and A. P. Dove, *Chem. Soc. Rev.*, 2010, **39**, 486−494; (c) J.-F. Carpentier, *Macromol. Rapid Commun*., 2010, **31**, 1696−1705.

13 (a) G. W. Coates, *Chem. Rev.*, 2000, **100**, 1223−1252; (b) L. Resconi, L. Cavallo, A. Fait and F. Piemontesi, *Chem. Rev*., 2000, **100**, 1253−1345; (c) M. Lamberti, M. Mazzeo, D. Pappalardo and C. Pellecchia, *Coord. Chem. Rev*., 2009, **253**, 2082−2097; (d) P. Corradini, G. Guerra, L. Cavallo, *Acc. Chem. Res*. 2004**, 37**, 231-241; (f) A. J. Teator, T. P. Varner, P.C. Knutson, C. C. Sorensen and F. A. Leibfarth, *ACS Macro Lett*., 2020, **9**, 1638−1654.

14 (a) F. A. Bovey and P. A. Mirau, *NMR of Polymers*; Academic Press: San Diego, CA, 1996; (b) H. N. Cheng In *Modern Methods of Polymer Characterization*; H. G. Barth, J. W. Mays, Eds.; John Wiley & Sons: New York, 1991; pp 409−493.

15 T. M. Ovitt and G. W. Coates, *J. Am. Chem. Soc.*, 2002, **124**, 1316−1326.

16 T. M. Ovitt and G. W. Coates, *J. Polym. Sci.: Part A: Polym. Chem*., 2000, **38**, 4686−4692.

17 A. Nachtergael, O. Coulembier, P. Dubois, M. Helvenstein, P. Duez, B. Blankert and L. Mespouille, *Biomacromolecules*, 2015, **16**, 507−514.

18 K. S. Egorova and V. P. Ananikov, *Organometallics*, 2017, **36**, 4071−4090.

19 G. M. Miyake and E. Y.-X. Chen, *Macromolecules*, 2011, **44**, 4116−4124.

20 R. Todd, G. Rubio, D. J. Hall, S. Tempelaar and A. P. Dove, *Chem. Sci.* 2013, **4**, 1092−1097.

21 K. Makiguchi, T. Yamanaka, T. Kakuchi, M. Terada and T. Satoh, *Chem. Commun.*, 2014, **50**, 2883−2885.

22 J. B. Zhu and E. Y. X. Chen, *J. Am. Chem. Soc.*, 2015, **137**, 12506−12509.

23 A. Sanchez-Sanchez, I. Rivilla, M. Agirre, A. Basterretxea, A. Etxeberria, A. Veloso, H. Sardon, D. Mecerreyes and F. P. Cossío, *J. Am. Chem. Soc.*, 2017, **139**, 4805−4814.

24 B. Orhan, M. J.-L. Tschan, A.-L. Wirotius, A. P. Dove, O. Coulembier and D. Taton, *ACS Macrolett*., 2018, **7**, 1413−1419.

25 S. Liu, H. Li and Z. Li, *ACS Macro Lett.*, 2018, **7**, 624−628.

26 L. Zhang, F. Nederberg, J. M. Messman, R. C. Pratt, J. L. Hedrick and C. G. Wade, *J. Am. Chem. Soc.*, 2007, **129**, 12610−12611.

27 J. Y. C. Lim, N. Yuntawattana, P. D. Beer and C. K. Williams, *Angew. Chem. Int. Ed.*, 2019, **58**, 6007−6011.

28 M. S. Zaky, A.-L. Wirotius, O. Coulembier, G. Guichard and D. Taton, *Chem. Commun.*, 2021, **57**, 3777−3780.

29 M. J.-L. Tschan, K. Delle Chiaie, P. Bexis, A. Heard and A. P. Dove, manuscript in preparation.

30 M. Bero, P. Dobrzyński and J. Kasperczyk, *J. Pol. Sci., Part A: Polym. Chem.*, 1999, **37**, 4038-4042.

31 (a) J. Zhang, J. Xiong, Y. Sun, N. Tang and J. Wu, *Macromolecules*, 2014, **47**, 7789−7796; (b) C. Chen, J. Jiang, X. Mao, Y. Cong, Y. Cui, X. Pan and J. Wu, *Inorg. Chem.*, 2018, **57**, 3158−3168; (c) X. Li, Z. Jia, X. Pan and J. Wu, Chem. Asian J., 2019, **14**, 662−669; (d) Y. Sun, J. Xiong, Z. Dai, X. Pan, N. Tang and J. Wu, Inorg. Chem., 2016, 55, 136-143.

32 J. Char, O. G. Kulyk, E. Brulé, F. de Montigny, V. Guérineau, T. Roisnel, M. J.-L. Tschan and C. M. Thomas, *C. R. Chimie*, 2016, **19**, 167−172.

33 X. Zhang, G. O. Jones, J. L. Hedrick and R. M. Waymouth, *Nature Chem.*, 2016, **8**, 1047−1053.

34 Z. Kan, W. Luo, T. Shi, C. Wei, B. Han, D. Zheng and S. Liu, *Front. Chem.*, 2018, 6:547.

35 N. Spassky, M. Wisniewski, C. Pluta and A. Le Borgne, *Macromol. Chem. Phys.*, 1996, **197**, 2627−2637.

36 (a) E. L. Whitelaw, G. Loraine, M. F. Mahon and M. D. Jones, *Dalton Trans.*, 2011, **40**, 11469−11473; (b) S. L. Hancock, M. F. Mahon and M. D. Jones, *Dalton Trans*., 2013, **42**, 9279−9285; (c) L. Britton, D. Ditz, J. Beament, P. McKeown, H. C. Quilter, K. Riley, M. F. Mahon and M. D. Jones, *Eur. J. Inorg. Chem.*, 2019, 2768−2773; (d) I. dos Santos Vieira, E. L. Whitelaw, M. D. Jones and S. Herres-Pawlis, *Chem. Eur. J.*, 2013, **19**, 4712−4716; (e) J. Beament, M. F. Mahon, A. Buchard and M. D. Jones, *Organometallics*, 2018, **37**, 1719−1724; (f) C. Nalonkhet, T. Nanok, W. Wattanathana, P. Chuawong and P. Hormnirun, *Dalton Trans*., 2017, **46**, 11013−11030; (g) E. D. Cross, L. E. N. allan, A.

Decken and M. P. Shaver, *J. Polym. Sci., Part A: Polym. Chem.*, 2013, **51**, 1137−1146; (h) Z. Sun, R. Duan, J. Yang, H. Zhang, S. Li, X. Pang, W. Chen and X. Chen, *RSC Adv.*, 2016, **6**, 17531−17538; (i) C. Bakewell, R. H. Platel, S. K. Cary, S. M. Hubbard, J. M. Roaf, A. C. Levine, A. J. P. White, N. J. Long, M. Haaf and C. K. Williams, *Organometallics*, 2012, **31**, 4729−4736; (j) M. Normand, V. Dorcet, E. Kirillov and J.-F. Carpentier, *Organometallics*, 2013, **32**, 1694−1709; (k) S. M. Kirk, H. C. Quilter, A. Buchard, L. H. Thomas, G. Kocok-Kohn and M. D. Jones, *Dalton Trans.*, 2016, **45**, 13846−13852; (l) P. McKeown, M. G. Davidson, J. P. Lowe, M. F. Mahon, L. H. Thomas, T. J. Woodman and M. D. Jones, *Dalton Trans*., 2016, **45**, 5374-5387; (m) W.-L. Kong and Z.-X. Wang, *Dalton Trans*., 2014, **43**, 9126−9135.

37 S. Tabthong, T. Nanok, P. Sumrit, P. Kongaeree, S. Prabpai, P. Chuawong and P. Hormnirun, *Macromolecules*, 2015, **48**, 6846−6861.

38 S. Gesslbauer, R. Savela, Y. Chen, A. J. P. White and C. Romain, *ACS Catal*., 2019, **9**, 7912−7920.

39 A. Pilone, K. Press, I. Goldberg, M. Kol, M. Mazzeo and M. Lamberti, *J. Am. Chem. Soc.*, 2014, **136**, 2940−2943.

40 (a) K. Press, I. Goldberg and M. Kol, *Angew. Chem. Int. Ed.*, 2015, **54**, 14858−14861; (b) R. Hador, A. Botta, V. Venditto, S. Lipstman, I. Goldberg and M. Kol, *Angew. Chem. Int. Ed.*, 2019, **58**, 14679−14685.

41 M. D. Jones, L. Brady, P. McKeown, A. Buchard, P. M. Schäfer, L. H. Thomas, M. F. Mahon, T. J. Woodman and J. P. Lowe *Chem. Sci*., 2015, **6**, 5034−5039.

42 P. McKeown, M. G. Davidson, G. Kocik-Köhn and M. D. Jones, *Chem. Commun.*, 2016, **52**, 10431−10434.

43 X. Pang, R. Duan, X. Li, C. Hu, X. Wang and X. Chen, *Macromolecules*, 2018, **51**, 906−913.

44 See for instance A. Friedrich, J. Eyselein, J. Langer and S. Harder, *Organometallics* 2021, **40**, 3, 448–457.

45 S. Abbina and G. Du, *ACS Macro Lett.*, 2014, **3**, 689−692.

46 H. Wang and H. Ma, *Chem. Commun*., 2013, **49**, 8686−8688.

47 H. Wang, Y. Yang and H. Ma, *Macromolecules*, 2014, **47**, 7750−7764.

48 H. Wang, Y. Yang and H. Ma, *Inorg. Chem.*, 2016, ***55***, 7356−7372.

49 P. Hormnirun, E. L. Marshall, V. C. Gibson, A. J. P. White and D. J. Williams, *J. Am. Chem. Soc.*, 2004, **126**, 2688−2689.

50 C. Kan, J. Hu, Y. Huang, H. Wang and H. Ma, *Macromolecules*, 2017, **50**, 7911−7919.

51 J. Hu, C. Kan, H. Wang and H. Ma, *Macromolecules*, 2018, **51**, 5304−5312.

52 C. P. Radano, G. L. Baker and M. R. Smith, *J. Am. Chem. Soc*., 2000, **122**, 1552−1553.

53 (a) R. Duan, C. Hu, X. Li, X. Pang, Z. Sun, X. Chen and X. Wang, *Macromolecules*, 2017, **50**, 9188−9195; (b) C. M. Manna, H. Z. Kaplan, B. Li and J. A. Byers, *Polyhedron*, 2014, **84**, 160−167; (c) O. J. Driscoll, C. K. C. Leung, M. F. Mahon, P. McKeown and M. D. Jones, *Eur. J. Inorg. Chem.*, 2018, 5129−5135.

54 C. M. Manna, A. Kaur, L. M. Yablon, F. Haeffner, B. Li and J. A. Byers, *J. Am. Chem. Soc*., 2015, **137**, 14232−14235.

55 P. Marin, M. J.-L. Tschan, F. Isnard, C. Robert, P. Haquette, X. Trivelli, L.-M. Chamoreau, V. Guérineau, I. del Rosal, L. Maron, V. Venditto and C. M. Thomas, *Angew. Chem. Int. Ed.*, 2019, **58**, 12585−12589.

56 B. L. Small and M. Brookhart, *J. Am. Chem. Soc.*, 1998**, 120**, 7143-7144.

57 P. Marin, M. J.-L. Tschan, P. Haquette, T. Roisnel, I. del Rosal, L. Maron and C. M. Thomas, *Eur. Polym. J.*, 2019, **120**, 109208.

58 (a) A. Amgoune, C. M. Thomas and J.-F. Carpentier, *Pure Appl. Chem*., 2007, **79**, 2013-2030 and references therein. (b) A. Amgoune, C. M. Thomas and J.-F. Carpentier, *Macromol. Rapid Commun*., 2007, **28**, 693-697. (c) P. L. Arnold, J.-C. Buffet, R. P. Blaudeck, S. Sujecki, A. J. Blake and C. Wilson, *Angew. Chem., Int. Ed*., 2008, **47**, 6033-6036.

59 C. Bakewell, T.-P.-A. Cao, N. Long, X. F. Le Goff, A. Auffrant and C. K. Williams, *J. Am. Chem. Soc.*, 2012, **134**, 20577−20580.

60 T.-P.-A. Cao, A. Buchard, X. F. Le Goff, A. Auffrant and C. K. Williams, *Inorganic Chemistry*, 2012, **51**, 2157−2169.

61 C. Bakewell, A. J. P. White, N. J. Long and C. K. Williams, *Angew. Chem. Int. Ed*., 2014, **53**, 9226−9230.

62 T.-Q. Xu, G.-W. Yang, C. Liu and X.-B. Lu, *Macromolecules*, 2017, **50**, 515−522.

63 D. Myers, A. P. J. White, C. M. Forsyth, M. Bown and C. K. Williams, *Angew. Chem. Int. Ed*., 2017, **56**, 5277−5282.

64 A. Stopper, T. Rosen, V. Venditto, I. Goldberg, M. Kol, *Chem. Eur. J.* 2017, **23**, 11540-11548.

65 M. D. Jones, S. L. Hancock, P. McKeown, P. M. Schäfer, A. Buchard, L. H. Thomas, M. F. Mahon and J. P. Lowe, *Chem. Commun*., 2014, **50**, 15967−15970.

66 (a) S. Fortun, P. Daneshmand and F. Schaper, *Angew. Chem. Int. Ed.* 2015, **54**, 13669−13672; (b) P. Daneshmand, A. van der Est and F. Schaper, *ACS Catal.*, 2017, **7**, 6289−6301; (c) P. Daneshmand, S. Fortun and F. Schaper, *Organometallics,* 2017, **36**, 3860−3877.

67 (a) Ahn, S. H.; Chun, M. K.; Kim, E.; Jeong, J. H.; Nayab, S.; Lee, H. *Polyhedron* **2017**, *127*, 51−58. (b) Cho, J.; Nayab, S.; Jeong, J. H. *Polyhedron* **2016**, *113*, 81−87. (c) Kwon, K. S.; Cho, J.; Nayab, S.; Jeong, J. H. *Inorg. Chem. Commun.* **2015**, *55*, 36−38.

68 A. Amgoune, C. M. Thomas, S. Ilinca, T. Roisnel and J.-F. Carpentier, *Angew. Chem. Int. Ed.*, 2006, **45**, 2782–2784.

69 M. Bouyahyi, N. Ajellal, E. Kirillov, C. M. Thomas and J.-F. Carpentier, *Chem. Eur. J.*, 2011, **17**, 1872–1883.

70 J. Fang, M. J.-L. Tschan, T. Roisnel, X. Trivelli, R. M. Gauvin, C. M. Thomas and L. Maron, *Polym. Chem.*, 2013, 4, 360–367.

71 N. Ajellal, G. Durieux, L. Delevoye, G. Tricot, C. Dujardin, C. M. Thomas and R. M. Gauvin, *Chem. Commun.*, 2010, **46**, 1032–1034.

72 M. Terrier, E. Brulé, M. J. Vitorino, N. Ajellal, C. Robert, R. M. Gauvin and C. M. Thomas, *Macromol. Rapid Commun.*, 2011, **32**, 215–219.

73 J. M. Fraile, J. I. García, C. I. Herrerías, J. A. Mayoral and E. Pires, *Chem. Soc. Rev.*, 2009, **38**, 695-706.

74 X. Tang and E. Y.-X. Chen, *Nature Comm.*, 2018, **9**, 1–11.

75 X. Tang, A. H. Westlie, L. Caporaso, L. Cavallo, L. Falivene and E. Y.-C. Chen, *Angew. Chem. Int. Ed*, 2020, **59**, 7881–7890.

76 X. Tang, A. H. Westlie, E. M. Watson and E. Y.-C. Chen, *Science*, 2019, **366**, 754–758.

77 J. W. Kramer, D. S. Treitler, E. W. Dunn, P. M. Castro, T. Roisnel, C. M. Thomas and G. W. Coates, *J. Am. Chem. Soc.*, 2009, **131**, 16042–16044.

78 C. G. Jaffredo, Y. Chapurina, S. M. Guillaume and J.-F. Carpentier, *Angew. Chem. Int. Ed.*, 2014, **53**, 2687–2681.

79 C. G. Jaffredo, Y. Chapurina, E. Kirillov, J.-F. Carpentier and S. M. Guillaume, *Chem. Eur. J.*, 2016, **22**, 7629–7641.

80 R. Ligny, M. M. Hänninen, S. M. Guillaume and J.-F. Carpentier, *Angew. Chem. Int. Ed.*, 2017, **56**, 10388–10393.

81 J.-B. Zhu and E. Y.-X. Chen, *Angew. Chem. Int. Ed.*, 2019, **58**, 1178–1182.

82 J. Kiriratnikom, C. Robert, V. Guérineau, V. Venditto and C. M. Thomas, *Front. Chem.* 2019, **7**, 301.

83 (a) T. Aida and S. Inoue, *J. Am. Chem. Soc.*, 1985, **107**, 1358−1364; (b) T. Aida, K. Sanuki and S. Inoue, *Macromolecules*, 1985, **18**, 1049−1055; (c) A. Takasu, M. Ito, Y. Inai, T. Hirabayashi and Y. Nishimura, *Polym. J.*, 1999, **31**, 961−969; (d) Z. Hua, G. Qi and S. Chen, *J. Appl. Polym. Sci.*, 2004, **93**, 1788−1792; (e) Y. Maeda, A. Nakayama, N. Kawasaki, K. Hayashi, S. Aiba and N. Yamamoto, *Polymer*, 1997, **38**, 4719−4725.

84 L. Fournier, C. Robert, S. Pourchet, A. Gonzalez, L. Williams, J. Prunet and C. M. Thomas, *Polym. Chem.*, 2016, **7**, 3700−3704.

85 A patent from J.P. Robin, N. Radosevic, J. Blanchard US 20120022250 A1 reported the use of less toxic but much more expensive carbodimidazole (CDI) as alternative to phosgene.

86 Q. Feng and R. Tong, *J. Am. Chem. Soc.*, 2017, **139**, 6177−6182.

87 Q. Feng, L. Yang, Y. Zhong, D. Guo, G. Liu, L. Xie, W. Huang and R. Tong, *Nature Comm.*, 2018, **9**, 1559.

88 Y. Sun, Z. Jia, C. Chen, Y. Cong, X. Mao and J. Wu, *J. Am. Chem. Soc.*, 2017, **139**, 10723–10732.

89 M. Li, Y. Tao, J. Tang, Y. Wang, X. Zhang, Y. Tao and X. Wang, *J. Am. Chem. Soc.*, 2019, 141, 281−289.

90 H. Fouilloux, C. M. Thomas, *Macromol. Rapid Commun.* 2021, **42**, 2000530.